

**Synthesis and Characterization of PEG-b-PLGA
Copolymer-Based Nano Formulations via Flash Nano
Precipitation**



By

Mahad Wahaj Nasir

(Registration No: 00000362962)

Department of Chemical Engineering

School of Chemical and Materials Engineering

National University of Sciences and Technology (NUST)

Islamabad, Pakistan

(2024)

Synthesis and Characterization of PEG-b-PLGA Copolymer-Based Nano Formulations by Flash Nano Precipitation



By

Mahad Wahaj Nasir

Registration No: 00000362962

This thesis is presented in partial fulfillment of the criteria for the degree of
Master of Science in
Chemical Engineering

Supervisor Name: Dr. Muhammad Bilal Khan Niazi

School of Chemical and Materials Engineering
National University of Science and Technology (NUST)

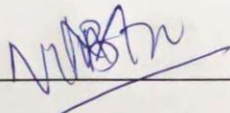
Islamabad, Pakistan

(2024)



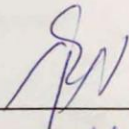
THESIS ACCEPTANCE CERTIFICATE

Certified that final copy of MS Thesis entitled "Synthesis and Characterization of PEG-b-PLGA Copolymer-based Nano Formulations via Flash Nano Precipitation" written by Mr Mahad Wahaj Nasir (Registration No 00000362962), of School of Chemical & Materials Engineering (SCME) has been vetted by undersigned, found complete in all respects as per NUST Statues/Regulations, is free of plagiarism, errors, and mistakes and is accepted as partial fulfillment for award of MS degree. It is further certified that necessary amendments as pointed out by GEC members of the scholar have also been incorporated in the said thesis.

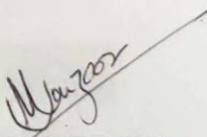
Signature: 

Name of Supervisor: Dr M. Bilal Khan Niazi

Date: 19/11/2024

Signature (HOD): 

Date: 06/01/2024

Signature (Dean/Principal): 

Date: 6/1/25



Form TH-1

National University of Sciences & Technology (NUST)

MASTER'S THESIS WORK

Formulation of Guidance and Examination Committee (GEC)

Name: Mahad Wahaj Nasir NUST Reg No: 00000362962
Department: Department of Chemical Engineering Specialization: Master of Science in Chemical Engineering
Credit Hour Completed: 18.0 CGPA: 3.75

Course Work Completed

S/No:	Code:	Title:	Core/Elective:	CH:	Grade:
1.	CHE-843	Separation Processes In Che	Compulsory	3.0	B+
2.	CHE-847	Chemical Kinetics& Reactor Design	Compulsory	3.0	B+
3.	RM-898	Research Methodology	Additional	2.0	Q
4.	ENE-809	Waste Water Treatment & Design	Elective	3.0	B+
5.	EME-921	Momentum, Heat & Mass Transfer In Chemical Engineering Separation Processes	Compulsory	3.0	A
6.	CHE-814	Product Technology	Elective	3.0	A
7.	ENS-830	Cleaner Production Technologies	Elective	3.0	A

Date 26 - Nov - 2022

Student's Signature

Thesis Committee

Name: Muhammad Bilal Khan Niazi (Supervisor)
Department: Department of Chemical Engineering
Name: Zakir Hussain (Cosupervisor)
Department: Department of Materials Engineering
Name: Zaib Jahan (Internal)
Department: Department of Chemical Engineering
Name: Asad Ullah Khan (Internal)
Department: Department of Chemical Engineering
Name: Muhammad Bilal Khan Niazi (External)
Department: Department of Chemical Engineering

Signature

Signature

Signature

Signature

Signature

Date: 26 - Nov - 2022

Signature of Head of Department:

APPROVAL



MASTER'S THESIS WORK

We hereby recommend that the dissertation prepared under our supervision by

Regn No & Name: 00000362962 Mahad Wahaj Nasir

Title: Synthesis and Characterization of PEG-b-PLGA Copolymer-based Nano Formulations via Flash Nano Precipitation.

Presented on: 25 Sep 2024 at: 1430 hrs in SCME Seminar Hall

Be accepted in partial fulfillment of the requirements for the award of Master of Science degree in **Chemical Engineering**.

Guidance & Examination Committee Members

Name: Dr Sulalit Bandyopadhyay (Norway)

Signature: Sulalit Bandyopadhyay

Name: Dr Asad Ullah Khan

Signature: Asad Ullah Khan

Name: Dr Zaib Jahan

Signature: Zaib Jahan

Name: Dr Zakir Hussain (Co-Supervisor)

Signature: Zakir Hussain

Supervisor's Name: Dr M. Bilal Khan Niazi

Signature: M. Bilal Khan Niazi

Dated: 05/11/2024

[Signature]

Head of Department

Date 08/11/24

[Signature]

Dean/Principal

Date 8/11/24

AUTHOR'S DECLARATION

It is confirmed that the MS Thesis entitled “Enhanced Bioelectricity Production in Microbial Fuel Cell Using Metal Organic Framework Based Anode” of Mr. Mahad Wahaj Nasir, Reg No. 00000362962 has been examined by me. I undertake that:

- a. Thesis has significant new work/knowledge as compared to already published or is under consideration to be published elsewhere. No sentence, equation, diagram, table, paragraph, or section has been copied verbatim from previous work unless it is placed under quotation marks and duly referenced.
- b. The work presented is original and own work of the author (i.e., there is no plagiarism). No ideas, processes, results, or words of others have been presented as the author's own work.
- c. There is no fabrication of data or results that the research is not accurately represented in the records. The thesis has been checked using TURNITIN (a copy of the originality report attached) and found within limits as per the HEC plagiarism Policy and instructions issued occasionally.

PLAGIARISM UNDERTAKING

I solemnly declare that research work presented in the thesis titled “Synthesis and Characterization of PEG-b-PLGA Copolymer-Based Nano Formulations via Flash Nano Precipitation” is solely my research work with no significant contribution from any other person. Small contribution/ help wherever taken has been duly acknowledged and that complete thesis has been written by me.

I understand the zero tolerance policy of the HEC and National University of Sciences and Technology (NUST), Islamabad towards plagiarism. Therefore, I as an author of the above titled thesis declare that no portion of my thesis has been plagiarized and any material used as reference is properly referred/cited.

I undertake that if I am found guilty of any formal plagiarism in the above titled thesis even after award of MS degree, the University reserves the rights to withdraw/revoke my MS degree and that HEC and NUST, Islamabad has the right to publish my name on the HEC/University website on which names of students are placed who submitted plagiarized thesis.

Student Signature: _____ Mahad Wahaj Nasir

DEDICATION

By the grace of Almighty Allah, who is the most Beneficent and the most Merciful.

This research is dedicated to my parents, who have always been my source of guidance and support.

To my supervisors who shared their knowledge, gave advice, and encouraged me to fulfill my tasks.

And to all my fellows, with whom I worked and shared good memories.

ACKNOWLEDGEMENTS

All praises to Almighty Allah, without His will, nothing can happen, who favored us with the capacity to think and made us anxious to investigate this entire universe. Incalculable greetings upon the Holy Prophet Hazrat Muhammad (PBUH), the reason for the creation of the universe and wellspring of information and blessing for whole of humankind.

From the core of my heart, I am thankful to my research supervisors, Dr. Muhammad Bilal Khan Niazi and Dr. Sulalit Bandyopadhyay for their unwavering technical and moral support enlightening me with a research vision and pushing me for excellence. Their quest for perfection and excellence had been a source of inspiration and a driving force. It's their consistency and encouragement that empowered me to achieve this onerous milestone.

I extend my sincere gratitude to my guidance and committee members: Dr. Zaib Jahan, Dr. Zakir Hussain, and Dr. Attaullah Khan for guiding and supporting me in my research course. It would not have been possible without them. I would also like to express my gratitude to Nesrine Bali for sharing her knowledge and experience.

I am thankful for My Seniors and colleagues who shared their knowledge regarding experimental techniques, and they motivated me in this entire research work. Without any doubt, IKP's supporting staff coordinated with me while I was working with different equipment.

I am highly obligated to my parents and siblings for their never-ending love. Thanks for believing in me, wanting the best of me, and inspiring me to follow my passion. To my friends Reema, Sarmad, Camillo, Felix, Hizbullah and Haroon, thank you for your support, advice, and encouragement.

Mahad Wahaj Nasir

TABLE OF CONTENTS

ACKNOWLEDGEMENTS.....	viii
LIST OF TABLES.....	xi
LIST OF FIGURES.....	xii
List OF SYMBOLS, ABBREVIATIONS AND ACRONYMS.....	xiii
ABSTRACT.....	xiv
CHAPTER 1: INTRODUCTION.....	1
1.1 Background.....	1
CHAPTER 2: LITERATURE REVIEW.....	6
2 Theory.....	6
2.1 Polymer.....	6
2.1.1 Polymer Synthesis.....	6
2.1.2 Step Growth Polymerization.....	8
2.1.3 Chain or Addition Polymerization.....	9
2.1.4 Free Radical Polymerization.....	9
2.2 Block Copolymers.....	10
2.2.1 Synthesis of Block Copolymers.....	11
2.2.2 Block Copolymer as Drug Delivery System.....	13
2.3 Flash Nano Precipitation (FNP).....	14
2.4 Nanoparticles.....	17
2.4.1 Polymeric Nanoparticles (PNPs).....	17
2.4.2 Iron Oxide Nanoparticles (IONPs).....	18
CHAPTER 3: METHODOLOGY.....	20
3 Materials and Methods.....	20
3.1 Materials.....	20
3.2 Methods of Synthesis.....	20
3.2.1 Synthesis of PEG-b-PLGA Copolymer.....	20
3.2.2 Synthesis of IONPs.....	22

3.2.3	Nanoparticle Formulations using Flash Nano Precipitation	22
3.3	Characterization Techniques.....	24
3.3.1	Nuclear Magnetic Resonance	24
3.3.2	Fourier Transform Infrared Spectroscopy (ATR-FTIR).....	26
3.3.3	X-ray Crystallography (XRD)	27
3.3.4	Scanning Transmission Electron Microscope (S(T)EM).....	28
3.3.5	Dynamic Light Scattering (DLS).....	29
3.3.6	Gel Permeation Chromatograph (GPC).....	30
CHAPTER 4: RESULTS AND DISCUSSION.....		32
4	Results and Discussion	32
4.1	Characterization of Polymers.....	32
4.1.1	Nuclear Magnetic Resonance (NMR)	32
4.1.2	Gel Permeation Chromatograph	33
4.1.3	Fourier Transform Infrared Spectroscopy (FTIR).....	34
4.2	Characterization of Iron Oxide Nanoparticles	35
4.2.1	X-ray diffraction spectroscopy	35
4.2.2	Transmission Electron Microscopy and Vibrating Sample Magnetometer (VSM) 36	
4.3	Nanoparticles Characterization Synthesized using MIVM.....	37
4.3.1	Sizes of Nanoparticles: Bare PNPs and PNPs incorporating IONPs.....	37
4.3.2	Fourier Transform Infrared Spectroscopy:	43
4.3.3	Scanning (Transmission) Electron Microscopy:.....	43
5	CHAPTER 5: CONCLUSIONS	48
5.1	Future Recommendations:	49
6	REFERENCES	50

LIST OF TABLES

Table 2.1: Synthesis routes for block copolymers	11
Table 4.1: Molar ratio of glycolide to lactide.....	33
Table 4.2: Molecular weights and polydispersity measured through GPC.....	34

LIST OF FIGURES

Figure 1.1: Encapsulation of iron oxide within the polymer nanosphere[22].	5
Figure 2.1: Classification of Polymers [25]	6
Figure 2.2: Step Growth Polymerization [28]	8
Figure 2.3: Addition Polymerization [29]	9
Figure 2.4: Schematics of copolymers [33]	10
Figure 2.5: Schematic representation of the nanoparticle formation process during the FNP.	15
Figure 2.6: Different mixer geometries are employed to create turbulent conditions with elevated rates of energy dissipation within a confined space. (a) confined impinging jets (b) Multi-Inlet Vortex Mixer with top and side views, and (c) Multi-Inlet Vortex Mixer [20]	16
Figure 3.1: Setup for the synthesis of PEGPLGA.	21
Figure 3.2: Setup for Iron oxide NPs synthesis.	22
Figure 3.3: (a) FNP setup with syringe pumps and (b)the main reactor for flash nanoprecipitation.	23
Figure 3.4: Graphics of the FNP Process	24
Figure 3.5: Working of NMR Spectroscopy	25
Figure 3.6: Working Mechanism of ATR-FTIR[79]	26
Figure 3.7: (a) Bruker D8 A25 DaVinci XRD (b) Schematic showing the main components of XRD	27
Figure 3.8: (a)High resolution S(T)EM Components (b) Schematic showing the main components of S(T)EM [83]	29
Figure 3.9: Anton Paar LiteSizer 500	30
Figure 3.10: Schematic diagram of the separation principle of gel permeation chromatography (GPC)	31
Figure 4.1: Proton nuclear magnetic resonance (¹ H NMR) spectra of mPEG-b-PLGA	33
Figure 4.2: FTIR spectra of PEG-PLGA copolymer with different MW mPEG initiators.	34
Figure 4.3: X-rays Diffraction Spectroscopy of IONPs	35
Figure 4.4: TEM image of Iron Oxide Nanoparticles with uniform size distribution.	36
Figure 4.5: Characterization of IONPs against applied field	37
Figure 4.6: Sizes of Bare PNPS (0.5,1 and 2 wt.%) vs. PNPs combined with IONPs (a,b) and Distribution (intensity%) plots from DLS data corresponding to the IONPs coated polymer data (c, d)	40
Figure 4.7: Stability of PNPs characterized by DLS	41
Figure 4.8: Comparison of colloidal stabilities for both (a,b)PEG ₂₀₀₀ PLGA and (c,d)PEG ₅₀₀₀ PLGA: Bare PNPs vs. PNPs incorporating IONPs	42
Figure 4.9: FTIR spectrums comparing bare PNPs vs PNPs-IONPs	43
Figure 4.10: SEM images of PEG ₂₀₀₀ PLGA (a) and PEG ₅₀₀₀ PLGA (b)	45
Figure 4.11: (a, b, c, d, e, f) TEM images showcasing the attachments of polymer with IONPs, and (g,h) EDX spectrum confirming iron oxide particles presence with the polymer	47

List OF SYMBOLS, ABBREVIATIONS AND ACRONYMS

NP	Nanoparticles
PNPs	Polymeric Nanoparticles
IONPs	Iron Oxide Nanoparticles
CIJ	Confined Impinging Jet
DCM	Dichloromethane
BCP	Block Copolymer
DLS	Dynamic Light Scattering
FNP	Flash Nanoprecipitation
FTIR	Fourier-Transform Infrared Spectroscopy
GPC	Gel Permeation Chromatography
LA	Lactic Acid
MIVM	Multi-Inlet Vortex Mixer
NMR	Nuclear Magnetic Resonance
PEG	Polyethylene Glycol
PEG-PLGA	Poly (ethylene glycol)-b-poly(lactic-co-glycolic acid)
PGA	Poly (Glycolic Acid)
PLA	Poly (Lactic Acid)
ROP	Ring Opening Polymerization
Sn(Oct) ₂	Stannous Octoate
S(T)EM	Scanning Transmission Electron Microscopy
THF	Tetrahydrofuran

ABSTRACT

Flash Nanoprecipitation (FNP) is a popular and straightforward technique that involves the assembly of amphiphilic copolymers into nanoparticles for biomedical applications. The method is economical and fast for the versatile structure of block copolymers and their ability to form nanoparticles. Medical grade nanoparticles offer unique opportunities, such as controlled drug release, imaging contrast agents, and hyperthermic cancer treatment. The objective of the study was to produce two types of nanoparticles via the FNP process, polyethylene glycol–poly lactic-co-glycolic acid (PEG-PLGA) nanoparticles with different molecular weights and PEG-PLGA coated iron oxide nanoparticles (IONPs).

The ring-opening polymerization (ROP) technique was used to successfully synthesize amphiphilic block-copolymers with hydrophilic PEG, and hydrophobic PLGA part. A standardized procedure was introduced to produce polymers with varying molecular weights. This involved using stannous octoate as a catalyst to get a 50:50 ratio of lactide to glycolide. The ratio of a PLGA copolymer promotes enhanced breakdown compared to a PLGA copolymer containing a higher quantity of either of the two monomers.

Following that, the development of targeted medicine delivery methods was conceptualized through the introduction of IONPs. The IONPs were synthesized by the utilization of a thermal decomposition process, using iron oleate as a precursor. This method resulted in the production of particles dispersed in tetrahydrofuran (THF) with a consistent size of 10-20nm, possessing magnetic characteristics.

Bare polymeric nanoparticles (PNPs) with sizes 80-160nm were formed by introducing amphiphilic block copolymer PEG-PLGA with different weight percentages in a solvent to a multi-inlet-vortex mixture (MIVM) without the use of a stabilizer. Another set of experiments was conducted in which IONPs were incorporated into the polymers to produce nanocarriers that were slightly bigger, but their particle stability over time increased. The effective attachment of IONPs within the polymer shell was verified using transmission electron microscopy (TEM). These nanocarriers should have the inherent potential of individual units to exhibit biodegradability, biocompatibility, and a good toxicological profile as further research is required for applicational prospects. Consequently, these engineered particles can serve as ideal carriers for diverse drug delivery applications, with polymers providing temporal control and iron oxide ensuring the treatment target specific.

CHAPTER 1: INTRODUCTION

1.1 Background

The fate of a medication delivery system that may effectively respond to external stimuli or internal signals originating from the target tissue has garnered significant attention in the field of research. A variety of physical and chemical stimuli present in the microenvironment or by external triggers, including but not limited to heat, magnetism, enzymes, and pH, can serve as potential triggers[1]. Nanoparticles play a key role in enhancing the efficacy of drug delivery systems, serving as both pharmacological agents and diagnostic tools[2]. Polymeric nanoparticles have been the subject of more and more research in the biomedical sciences in recent years. Polymer-based nanoparticles have been applied in devices, tissue-engineered scaffold design, cancer therapy, clinical bioanalytical diagnostics, and site-specific delivery[3]. These nanoparticles offer an array of options for targeted administration, including the delivery of hydrophobic medicines, macromolecules, and vaccinations to cells and organs such as the liver, brain, and lungs. However, a nanoparticle needs to have certain essential characteristics, like drug compatibility, biocompatibility, and appropriate biodegradation kinetics, to be used as a vector for drug delivery systems (DDSs)[4].

The Food and Drug Administration (FDA) has mandated since 1990 that these materials must exhibit biocompatibility, appropriate biodegradation kinetics, favourable toxicological profile and efficient drug-loading capabilities[5]. These particles can be classified as natural or synthetic based on the type of polymer employed in their formation. In recent decades, there has been a growing utilization of synthetic biodegradable polymers, such as polyamides, polyesters, poly (amino acids), and polyurethanes. This trend can be attributed to their advantageous characteristics, namely their ability to be manipulated in terms of molecular weight and structure, including linear, branching and dendritic configurations.

The goal of drug delivery is to deliver drugs to their target site of action in a precise and controlled manner, potentially improving their effectiveness and ensuring their safety. This approach aims to enhance the therapeutic effectiveness of the drugs, while simultaneously reducing the required dosage and limiting any undesired side effects. During the synthesis and design of the nanoparticles, aspects including particle size, surface characteristics, and release rate can be controlled for a therapeutically optimal dosing and site-specific effect of the drug.

PNPs have also been identified as highly advantageous vehicles for drug delivery owing to their adjustable properties, diminutive size below 1 μm , and the potential to encapsulate, dissolve, or interact with drug molecules or other active compounds through the utilization of polymeric nanocarriers[3]. The main challenges associated with traditional medicine are the inadequate solubility of medications in water, resulting in low absorption rates by the body, limited in vivo lifespan due to rapid clearance, and the occurrence of undesirable side effects[6]. Because of their sub-micron dimensions and hydrophilic nature, it is possible for PNPs to effectively traverse tissues by passing through capillaries and ultimately reaching the desired target region, where they can be captured by cells. The control of nanoparticle size is of utmost importance in drug delivery applications, as it directly impacts the biodistribution profile. This phenomenon is organ-specific and does not follow a linear pattern to size. Smaller nanoparticles, with a mean diameter of less than 60-70 nm, are rapidly excreted, on the other hand, the liver and spleen can filter out bigger nanoparticles that are larger than 200 nm. Consequently, for in vivo use, nanoparticles having diameters between 70 and 200 nm are crucial.[7].

Among the several options considered, poly (lactic-co-glycolic acid) (PLGA) has gained significant recognition in the field of medicine due to its extensive use as a material for biodegradable sutures. Despite the ability to manipulate several characteristics of PLGA nanoparticles, such as their size and morphology, by parameter (monomer ratio of individual monomer used, time and temperature of copolymerization reaction) adjustments during synthesis, some unresolved issues persist in the utilization of pure PLGA mainly detected by the body's reticuloendothelial system[8].

On the other hand, polyethylene glycol (PEG) is frequently employed in medicine for many purposes. It is administered orally as a laxative, utilized in medication formulation, and applied in capsule manufacture as a coating agent[9]. In the year 1990, the approval of PEGylated adenosine deaminase marked the introduction of the first polymer protein conjugate in the United States[10]. PEG is a hydrophilic and non-biodegradable polyether. This non-biodegradability enhances its biocompatibility as there is no accumulation and it is eliminated unchanged by the kidneys, particularly for low molecular weight chains. Due to its hydrophilicity, PEG polymer can stabilize nanoparticles in aqueous fluids and prevent aggregation through steric hindrance during application. It has established itself as an important in vivo half-life prolongation, and reduction of aggregation in the field of drug delivery. The

primary advantage of PEG would be its ability to deal with opsonization phenomena which refers to the rapid identification of foreign entities, including pathogens, pharmaceuticals, and nanoparticle devices, by the immune system. This significant milestone, together with the potential to address many challenges associated with polymers in drug delivery, has led to a substantial increase in attention to PEG.

In order to make PLGA more stealthy and avoid detection by the body's reticuloendothelial system, PEG coatings were first introduced in 1994[11]. The study highlighted that a significant increase in the half-life of nanoparticles occurred when they were coated with PEG polymer. It was clear that PEG coating on the core must exhibit stability under both in vitro and in vivo settings. Furthermore, this ability of PEG to extend the circulation of drugs demonstrated greater efficacy when covalently bonded as compared to simple adsorption on the surface[12]. To harness these benefits, a PEG-PLGA copolymer is considered one of the best organic carriers because of its ease of synthesis. It has not only the ability to bring the desirable qualities of both PEG and PLGA but also has distinct properties because of its well-defined hydrophilic part (PLGA) and its hydrophilic one (PEG). These attributes make the PLGA-b-PEG an amphiphilic polymer. It was first synthesized in 1994 through covalent linkage. Because of these attributes, PEG-PLGA copolymer nanoparticles have been widely studied as pharmaceutical goods and in drug delivery applications. Various investigations have been done about the types of block copolymer, whether di, tri, or multiblock copolymer as well as linear or branched. Furthermore, functionalization with ligands has also shown promise in delivering drugs at specific sites. Among different variations, the di-block copolymer is the most encouraging because of its unique property of amphiphilicity and simplified synthesis when compared to other copolymers[13]. So in this study, we have focused on the synthesis and characteristics of di-block copolymers.

Several methods have been dedicated to the fabrication of nanoparticles laden with drugs, with the aim of enhancing medication delivery. Various methods are available to create PNPs, from emulsion polymerization to solvent displacement method, with nanoprecipitation being the contemporary one. Nanoprecipitation is one of the most effective methods for synthesizing PNPs and loading drugs. The term nanoprecipitation was initially introduced in 1989[14] and is sometimes referred to as de-solvation, antisolvent precipitation, and solvent displacement. Hydrophobic medicines, polymers, hydrophobic proteins, and other hydrophobic components have all been created with the use of nanoprecipitation. It has been estimated that 90% of

medications under development and 40% of pharmaceuticals with clinical approval are hydrophobic and poorly soluble in water. As a result, nanoprecipitation is an effective technique for creating these hydrophobic medications. Drugs can have their release kinetics controlled, and their chemical stability enhanced by being formulated into nanoparticles. Traditional medicine have a tendency to clump together, so these medications are typically coprecipitated with surfactants, polymers, or lipids to stabilize the particles by supplying a steric stabilizing layer[15]. In the nanoprecipitation method, hydrophobic entities are dissolved in water-miscible solvents. These solvents like tetrahydrofuran (THF), dimethyl sulfoxide (DMSO), or acetone usually provide high solubility for hydrophobic solutes. When this solution is combined with a significant quality of antisolvent, water, or buffer solution, hydrophobic solutes precipitate out due to declined solubility. Conventional nanoprecipitation typically involves adding antisolvents to solvents containing hydrophobic molecules drop by drop in a bulk solution while mixing[16]. This mixing step in the traditional method puts a limitation on its effectiveness and can cause wide particle size distribution[17]. To remedy this flash nanoprecipitation (FNP), initially pioneered by Brian K. Johnson and Robert K. Prud'homme, introduced a specific mixing chamber for the solvent and the anti-solvent. Designed as a controlled and scalable precipitation technique, its purpose is to produce a mixing time that is less than the nucleation and growth time of a nanoparticle[18, 19]. The basic setup involves the introduction of solvent and antisolvent into a specialized reactor at high velocities and a brief mixing duration of milliseconds, with two or more inlets. Currently, there are two types of reactors being used: the multi-inlet vortex mixer (MIVM) and the confined impinging jet (CIJ). The difference between the two processes involves the number of inlets and flow rates. As CIJ has the limitation of two inlets with identical flow rates, the MIVM can overcome the constraints by incorporating more inlets into the design, by adjusting the solvent: anti-solvent ratio, and by varying flow rates[20].

This study aims to analyze the benefits of utilizing PLGA-b-PEG copolymer for the creation of stable, precisely defined nanoparticles through FNP while employing MIVM. These nanocarriers can be used for various drug delivery purposes. Using a MIVM, PLGA being more hydrophobic goes to the inside while PEG comes outside in a core-shell arrangement, providing stability to the nanocarriers. Further improvements in drug delivery have been made by using magnetite as a drug-releasing carrier at specific sites by applying a magnetic field. It is crucial to understand the significance of adding magnetic nanoparticles (MNPs). The

addition of IONPs will help in achieving rapid and effortless magnetic separation. To achieve a high level of control over the size, shape, and morphology of particles, as well as their magnetic characteristics, we have created iron oxide nanoparticles (IONPs) by the thermal decomposition method[21].

In this work, we have first synthesized PEG-b-PLGA copolymer with PEG as more hydrophilic than PLGA. Two different molecular weights of PEG have been used as precursors and macroinitiators. The incorporation of iron oxide nanoparticles (IONPs) within polymeric nanoparticles has been successfully achieved through the implementation of flash nanoprecipitation in the dual inlet vortex mixer. The NPs were subjected to characterization using DLS (Dynamic Light Scattering) in order to document the changes in size and zeta potential of the NPs based on the polymer's molecular weight and starting concentration. Previous studies employing flash nanoprecipitation for PEG-PLGA synthesis posed problems with nanoparticle stabilities[15]. Here we have also discussed part stability using DLS characterization as to how the inclusion of PEG reduces aggregations. In addition, it is important to regulate the charged surface of nanoparticles to counter the accumulation of particles. The aggregation potentials of colloidal suspensions were evaluated using the zeta potential with pH, which measures the electric potential at the hydrodynamic layer's surface. Particles that had strongly negative, or positive zeta potential values tend to repel one another. The process mitigates aggregation while preserving their form and structural integrity. The potential for magnetic properties of the nanoparticles has also been studied. Additionally, in light of the impacts that have been noticed, various adjustments to the parent process are also examined, and suggestions are made for future work to fulfill the project's ultimate goal.

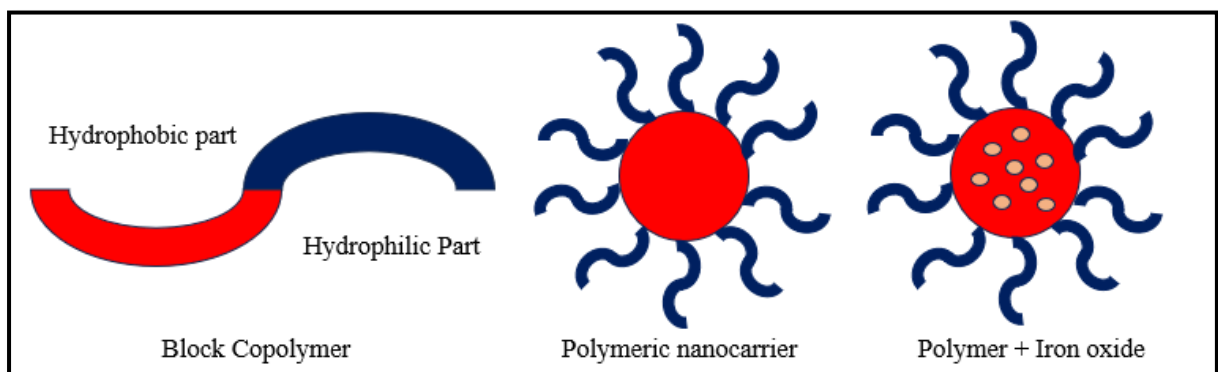


Figure 0.1: Encapsulation of iron oxide within the polymer nanosphere[22].

CHAPTER 2: LITERATURE REVIEW

Theory

2.1 Polymer

Berzelius coined the term "polymer" about a century ago to acknowledge that two compounds can have identical compositions but varying molecular weights. He categorized polymerism as a distinct form of isomerism[23]. Polymers are formed via the polymerization of several smaller molecules, resulting in the creation of macromolecules. Monomers refer to the small molecules that mix with each other to form polymer molecules, while the process of their combination is known as polymerization. A polymer molecule can consist of several monomer molecules, ranging from hundreds to perhaps tens of thousands or more. Types of polymers, from natural to synthetic are shown in Figure 2-1. Polymers refer to materials with molecular weights that can range from hundreds of thousands to millions[24].

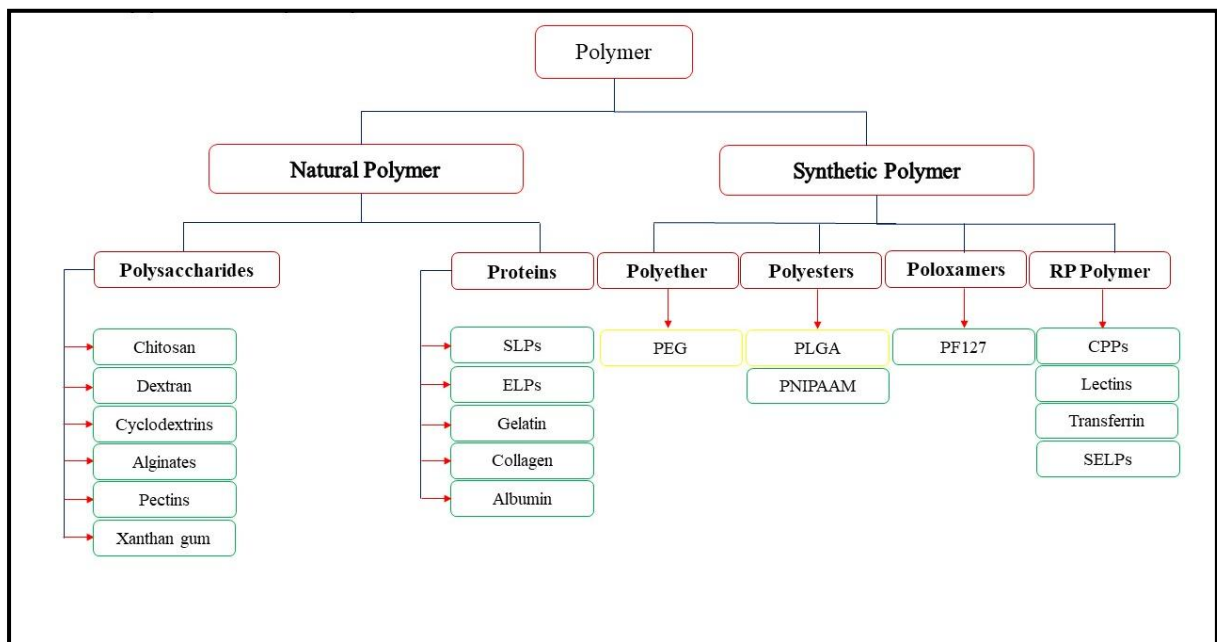


Figure 2.1: Classification of Polymers [25]

2.1.1 Polymer Synthesis

The initiation of polymerization reactions occurs when monomer molecules are added to active propagation centres. This addition is achieved by the production of additional bonds, resulting in the creation of a macromolecule with a high molecular weight. Polymerization is a complex process that involves multiple steps, resulting in the presence of non-uniform chain lengths in

each polymer. The degree of polymerization often corresponds to the number of monomer units present in a macromolecule. A key characteristic that differentiates a synthetic polymer from a simple molecule is the impossibility of determining an exact molar mass for a polymer. The length of the chain produced in a polymerization operation is solely dictated by random occurrences. A condensation reaction relies on the presence of an appropriate reactive group, whereas an addition reaction depends on the stability of the chain carrier. The objective in these cases is to narrow the distribution. Accurate regulation of molecular weight distributions can be attained by carefully controlling the initiator concentration and reaction duration.

Monomers exist which contain charges both negative and positive separately as well as combined and this forms their structure. Various polymerization methods exist based on the mechanism of polymerization, including ionic (anionic polymerization), radical polymerization, live anionic polymerization, cationic polymerization, ring-opening polymerization, multimode polymerization, and coordination polymerization. The primary techniques of polymerization, commonly employed in commercial applications, include ionic (both cationic and anionic), radical, and coordination polymerization. Living radical polymerization and ring-opening polymerization are contemporary techniques that show great potential in producing innovative goods. It is convenient to broadly classify polymerization reactions based on the mechanism of polymerization mentioned previously into two or three fundamental categories. Condensation and addition polymerization are the primary methods of polymerization, including many polymerization processes with only a few exceptions. During condensation polymerization, the polymer's chemical repeat unit has a distinct molecular formula from the monomer that forms it.

The addition polymerization possesses identical molecular formula as their monomers, serving as their structural unit. A common example of this type of addition polymerization is the production of polystyrene from styrene, where the resulting polymer has identical repeating units as the monomer used to form the polymer. Nevertheless, certain polymerization reactions do not readily align with these established categories. The synthesis of polyurethanes from isocyanates and alcohols involves a condensation polymerization process that does not involve the removal of water molecules from the final product. Similarly, certain ring-opening polymerization reactions are considered to yield products that can also be obtained using condensation polymerization, which is a type of addition polymerization. Polymerization can be classified into two main types based on the chemical process by which polymer chains are

extended: step-growth, which includes polycondensation, and addition/chain polymerization[26].

2.1.2 Step Growth Polymerization

Step growth polymerization is a polymerization process that produces dimers, trimers, longer oligomers, and long-chain polymers by combining bifunctional or multifunctional monomers. Step growth polymerization is responsible for the production of numerous naturally occurring and manufactured polymers. Polymers such as polyesters, polyamides, and polyurethanes are formed by the step-growth polymerization method. Due to the sequential nature of step-growth polymerization, a significant degree of reaction is necessary to attain a substantial molecular weight.

Polymerization occurs when individuals are periodically instructed to interlock their hands with their closest neighbor. Initially, only individuals in pairs can be found in the field. Once enough time had passed, every available hand could have been connected, resulting in the entire crowd forming a single unbroken human chain, resembling a macromolecule chain. Figure 2-2 depicts a schematic representation of an LSGP architecture. The unfilled dots symbolize bifunctional monomers, whereas the interconnected black dots indicate the developing polymeric oligomers. Over extended time periods, extremely massive macromolecules become prevalent, while only a small number of monomeric species remain[27].

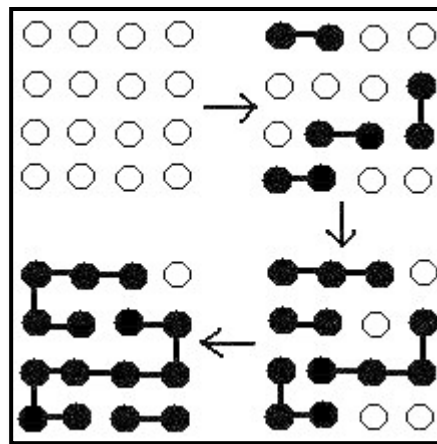


Figure 2.2: Step Growth Polymerization [28]

2.1.3 Chain or Addition Polymerization

When addition polymerization, sometimes referred to as chain-growth polymerization, occurs, a series of chemical reactions occurs where new monomer units are added to the polymer molecule as it grows. This is accomplished by creating two or three bonds with the monomer. The process of polymerization happens in several phases:

- Chain initiation: Typically accomplished through the use of an initiator that initiates the polymerization process. In the cases of free radical polymerization, cationic polymerization, anionic polymerization, and coordination polymerization, the reactive start molecule may take the shape of a radical, cation, anion, or organometallic complex.
- Chain propagation: A monomer attaches to the chain, and each subsequent monomer unit generates a reactive site for the following attachment.
- Chain termination: It's the stopping of the chain's propagation due to the neutralization of the radical, cation, or anion.

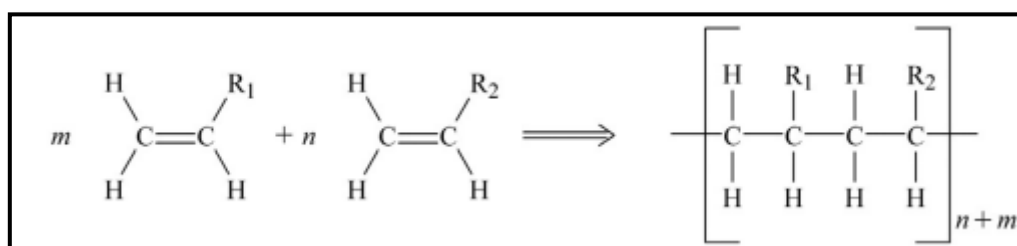


Figure 2.3: Addition Polymerization [29]

2.1.4 Free Radical Polymerization

The term "polymerization" refers to the process of creating a polymer from a monomer. "Free-radical addition polymerization," sometimes referred to as "radical polymerization," is the process of chain polymerization using unsaturated monomers and free radicals acting as a chain carrier.

Historically, it is believed that the presence of an impurity (peroxide) in benzaldehyde inadvertently catalyzed a reaction, leading to the occurrence of free radical polymerizations. These species are referred to as initiators because they commence polymerization by decomposing and producing radicals. The mechanism of these radical-initiated

polymerizations corresponds to the method for addition polymerization. The free radicals initiate and propagate the quickly expanding chains. The reaction terminates when the two radicals encounter each other through random collisions[30].

2.2 Block Copolymers

Copolymers consist of distinct monomer units and are classified into random, alternating, block, and graft copolymers. Random copolymers are copolymers that consist of repeated units arranged statistically along their backbone. The chance of a specific monomer unit occurring at a particular position is not influenced by the kind of neighboring units[31]. Monomers in alternating copolymers are copolymerized along the chain in a regular, alternating sequence. A polymer chain serves as the graft copolymer's backbone, while side polymer chains are joined by covalent bonds to form the branches. Chemically bonded homopolymers known as block copolymers are arranged according to the sequential sequence of their component segments. Because of their amphiphilic characteristic, which is the ability of a hydrophilic block to chemically bond with a hydrophobic block, they have found extensive use in pharmaceutical applications[32]. Block copolymer designs incorporating A, B, and C monomer units are shown in Figure 2-4. The A-B unit, segments of two different homopolymer fragments that make up the AB di-block type, is the most basic linear block copolymer. A tri-block copolymer known as ABA is formed when the terminals of the B and A units are linked together. In multi-block copolymers, A and B segments are linked repeatedly with C units positioned in between. The nonlinear block copolymers include miktoarm star, graft, and star.

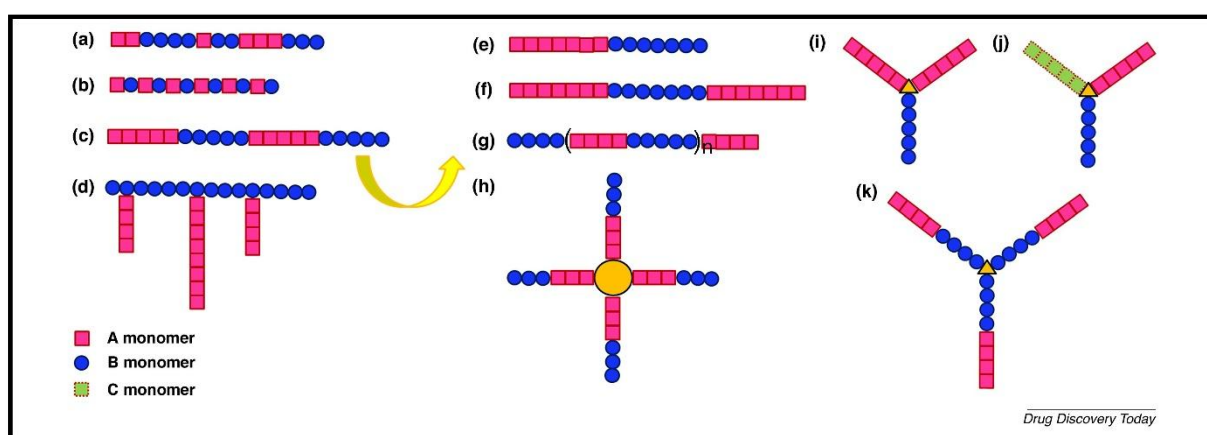


Figure 2.4: Schematics of copolymers [33]

Drug delivery methods have made substantial use of amphiphilic block copolymers, particularly in the micelle formulation. Amphiphilic BCPs are widely used in biomedical applications because of their chemical versatility, which consists of a hydrophilic block connected to a hydrophobic block. This adaptability allows for a wide range of applications. The length and molecular weight of both the hydrophilic and hydrophobic segments can be readily modified to attain the desired hydrophilic-lipophilic balance in the system. These copolymers allow for the selection of suitable copolymers to extend the duration of circulation, achieve selective targeting, and alter the drug-release characteristics of delivery mechanisms like micelles [34, 35].

2.2.1 Synthesis of Block Copolymers

The design of block copolymers has greatly advanced due to the progress achieved in anionic, radical, cationic, ring-opening, photo, and group-transfer polymerization processes.

Table 2.1: Synthesis routes for block copolymers

Synthesis Method	Overview
Synthesis by sequential living polymerization	<ul style="list-style-type: none"> <li data-bbox="596 1182 1391 1608">• The sequential addition of monomers in living anionic polymerization is a very effective method that allows for the production of copolymers with predictable molecular weight distributions. Complete conversion is accomplished using the synthetic method, which does not involve chain transfer or termination. Nevertheless, the sequence of monomer incorporation has significance in this method[36]. <li data-bbox="596 1626 1391 1937">• The utilization of living cationic polymerization allows for the production of polymers with precise and narrow molecular weight distribution. The polymerization process consists of the formation and growth of cationic propagating species. This process is distinguished by its precise and controlled initiation and propagation, to

	<p>minimize side-reaction termination and chain transfer. Isobutylene, vinyl ethers, and styrene are the most common monomers used in this form of polymerization[37].</p>
Controlled and living radical polymerization	<ul style="list-style-type: none"> • Despite its simplicity, free-radical polymerization is limited by the wide molecular weight dispersion of the polymers it produces. Ionic polymerization is highly advantageous for the production of block copolymers with precise MW architecture. However, its applicability is limited to a subset of functional monomers. Controlled or living radical polymerization (CRP/LRP) is the most adaptable method to create block copolymers. This is mainly because it can create copolymers with regulated molecular weight, molecular weight distribution, and functionality. It can also operate with a wide variety of monomers and impurities and its experimental requirements are less stringent[38].
Group transfer Polymerization (GTP)	<ul style="list-style-type: none"> • Group transfer polymerization has mostly been utilized for the synthesis of alkyl methacrylate-based block copolymers through successive monomer addition. The compounds with silyl ketene acetal functions as an initiator. The silane group is moved to the growing chain end at each addition step, guaranteeing that the chain end stays active until all of the monomer is consumed. By varying the amount of the initiator and monomer used, the molecular weight of the synthesized polymer may be predicted[39].
Ring Opening Polymerization (ROP)	<ul style="list-style-type: none"> • Ring-opening polymerization (ROP) is a type of polymerization process in which a reactive centre at the terminal end of a polymer chain facilitates the reaction with cyclic monomers by opening their ring structure, resulting in the formation of a lengthy polymer chain. The

	<p>propagating center can have a radical, anionic, or cationic character. Polymers with a density equal to or lower than that of the monomers can be synthesized using radical ring-opening polymerization ROP. ROP can provide polymers with functional groups such as ethers, esters, amides, and carbonates[40].</p>
--	---

2.2.2 Block Copolymer as Drug Delivery System

The development of polymer-based DDS has been the focus of an increasing amount of research in recent years. Block length ratios, hydrophilicity, solubility, physicochemical characteristics, amphiphilic behavior, and the incorporation of additional blocks with desired traits are among the intrinsic changes that these special block copolymers display. Block-copolymer-based nanostructures offer several benefits, such as the capacity to adjust their lipophilicity, transport both hydrophobic and hydrophilic pharmaceuticals, control the release of drugs, prolong blood circulation, minimize toxicity, and boost therapeutic efficacy[41].

2.2.2.1 Synthesis of block copolymers for drug delivery applications

Approximately 30–40% of novel drug candidates exhibit inadequate water solubility, posing challenges in formulating appropriate preparations [42]. Amphiphilic polymer-carriers show great promise for the delivery of hydrophobic drugs and can be further designed to positively affect the biodistribution of the encapsulated drug. The incorporation of hydrophilic polymers into medications can enhance solubility while a hydrophilic polymeric coating may increase the bioavailability of many medications [43]. These block copolymers are carefully synthesized into nanoparticles with specific sizes and types which are significantly influenced by the procedure conditions and the polymer utilized [44]. These nanocarriers show properties replicating their parent polymers. Almost all BCPs can be used to form nanoparticles but the copolymer synthesized should have certain unique properties like bioavailability, biocompatibility and a good toxicological profile to be used for drug delivery applications. A certain number of BCPs that fit the criteria and are being actively studied are polyethylene glycol-b-polystyrene (PEG-b-PS), polyethylene glycol-block-poly(ϵ -caprolactone) (PEG-b-PCL), Polyethylene glycol-block-poly(D,L-lactic acid) (PEG-b-PLA), and polyethylene

glycol–poly lactic acid-co-glycolic acid (PEG–PLGA)[45-47]. Among the BCPs extensively studied, Pustulka, K.M. highlighted that poly(ethylene glycol)-b-poly(lactic-co-glycolic acid) (PEG-b-PLGA) has shown the greatest suitability for prospective drug delivery applications owing to its capacity to generate stable nanoparticles, their biocompatibility, and their degradability[48, 49]. A diblock, triblock, or multiblock copolymer can be synthesized based on the quantity of blocks. The di-block copolymer is the most encouraging because of its unique property of amphiphilicity and simplified synthesis. Because of amphiphilicity (e.g., one hydrophilic and the other more hydrophobic), differential solubility of the blocks results in facilitating the self-assembly of polymer into nanoparticles[50]. In the self-assembly process, PLGA being more hydrophobic goes to the inside while PEG comes outside in a core-shell arrangement, providing stability to the nanocarriers.

Synthesise of PEG-PLGA di-block copolymers is commonly done using stannous octoate ($\text{Sn}(\text{Oct})_2$) as a catalyst. $\text{Sn}(\text{Oct})_2$ is the favored catalyst for the bulk synthesis of PLA, PLGA, and PCL in industrial and research applications. The use of $\text{Sn}(\text{Oct})_2$ as a catalyst is done to get a 50:50 ratio of lactide to glycolide. This ratio of a PLGA copolymer promotes enhanced breakdown compared to a PLGA copolymer containing a higher quantity of either of the two monomers[51]. In the synthesis of PEGPLGA block copolymer, the use of $\text{Sn}(\text{Oct})_2$ as a catalyst gives you control over the molecular weight distributions(a fixed polydispersity range) and the rate of reaction. Along with the catalyst they are also dependent on the amount of initiators, monomer concentration, temperature, and reaction time[52]. The quantity of initiator dictates the molecular weight of the resultant polymer. During polymerization, the quantity of D,L-lactide in the chain increases as the concentration of free glycolide monomers in the bulk diminishes[53, 54].

2.3 Flash Nano Precipitation (FNP)

Numerous techniques have been employed for the synthesis of PNPs to improve therapeutic delivery. Polymeric nanoparticles (PNPs) can be synthesized through the direct polymerization of monomers (e.g., emulsion polymerization, surfactant-free emulsion polymerization, mini-emulsion polymerization, micro-emulsion polymerization, and microbial polymerization) or by dispersing preformed polymers (e.g., nanoprecipitation, emulsification solvent evaporation, emulsification solvent diffusion, and salting-out)[55]. Among all the available methods the

FNP method provides a simple rapid one-step synthesis of homogenous nanoparticles process with greater flexibility and straightforward incorporation of drugs[56].

Flash Nano Precipitation (FNP) has been a highly adaptable technique during the past 20 years for generating polymer nanoparticles. FNP was initially documented by Johnson and Prud'homme in 2003[45]. It may be used with various hydrophobic polymers, block copolymers, and their combinations, and can also incorporate both organic and inorganic compounds. By selecting specific polymer(s), FNP can produce accurate formations with adjustable sizes and tight size distributions[57]. The dimensions of NPs can be regulated by manipulating the rates of solute nucleation and growth in solvent precipitation processes[20]. In an FNP method, the mechanism involves the rapid merging of a solution containing a solute in an organic solvent with an anti-solvent within a limited space (reactor) that is miscible with the organic solvent but acts as a non-solvent for solutes.

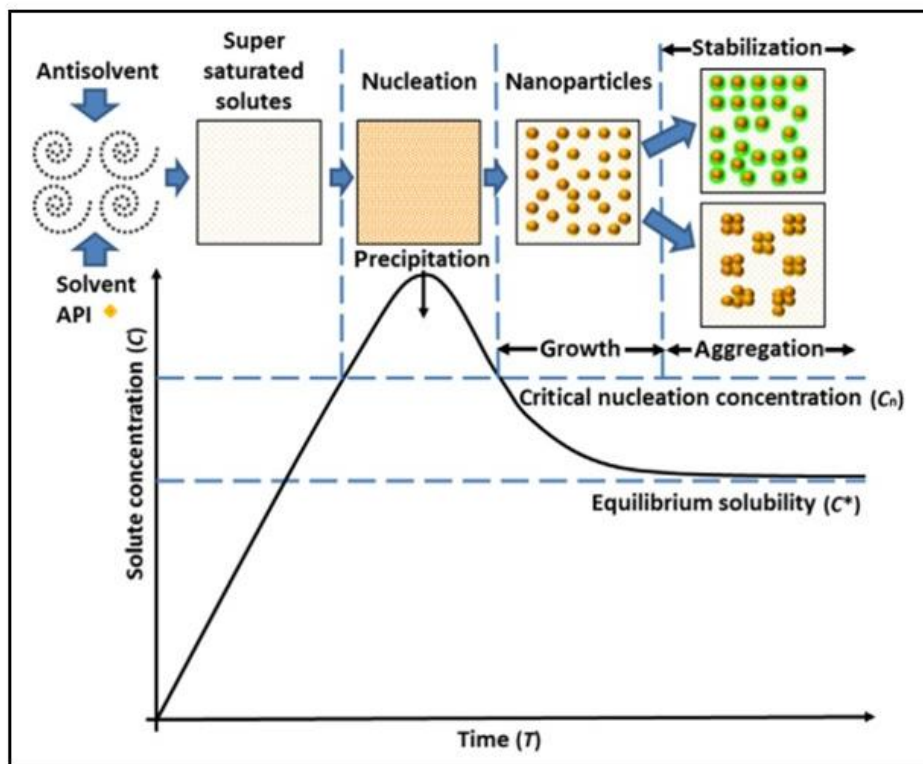


Figure 2.5: Schematic representation of the nanoparticle formation process during the FNP[18].

Within the reactor rapid turbulent mixing occurs, leading to local supersaturation, high rates of energy dissipation, and creating the necessary circumstances for both the solute and stabilizer to precipitate simultaneously [58]. The block copolymer hinders the continued enlargement of the solute particles and offers stabilization utilizing the hydrophilic block on the particle's surface. Different steps through the FNP process are depicted in Figure 2-5 [45]. Parameters like as flow rates and solvent/anti-solvent ratios directly affect the resultant nanoparticle sizes. The dissolved hydrophobic components precipitate as a result of supersaturation brought on by the fast and turbulent mixing of the organic solvent stream with water [49]. Some other factors affect the particle size and size distributions of PNPs. Y. Liu et al[15] demonstrated that the concentration of the polymer in the solvent affects the sizes of the resultant polymeric nanoparticles. As the polymer concentration increases, supersaturation increases so does the nucleation rate. Similarly, an increase in the molecular weight of polymers positively affects the sizes of nanoparticles.

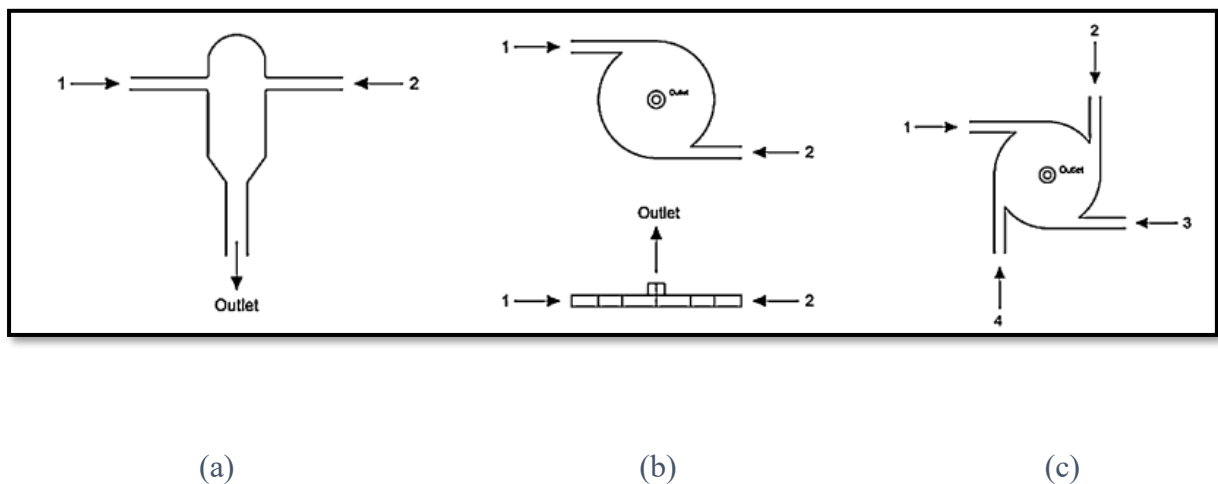


Figure 2.6: Different mixer geometries are employed to create turbulent conditions with elevated rates of energy dissipation within a confined space. (a) confined impinging jets (b) Multi-Inlet Vortex Mixer with top and side views, and (c) Multi-Inlet Vortex Mixer [20]

The utilization of two types of geometries has been extensive: confined impinging jets (CIJ) mixer and multi-inlet vortex mixer (MIVM) in the field of flash nanoprecipitation. The original CIJ mixer was developed with a confined mixing chamber and two opposing jets. The collision between two jets travelling at high speeds causes rapid micromixing of the fluids, leading to turbulent flow inside the mixing chamber. Johnson and Prud'homme observed a transition from a laminar flow to a turbulent-like flow when the Reynolds number (Re) reached roughly 90.

The micromixing period was exceptionally brief, with a duration of about a few milliseconds. Furthermore, the CIJ mixer efficiently controls the degree of supersaturation in medications or polymers by employing diverse organic solvents and nonsolvent (water) and modifying flow rates. This enables meticulous regulation of the resultant particle size[45, 59]. Nevertheless, the comparable speed at which the solvent and antisolvent move restrict their practical uses due to the possibility of a significant concentration of solvent in the end product, which might potentially undermine the quality and durability of the formed nanoparticles.

To address the constraint of requiring equal velocities for the opposing jets, a Multi-Inlet Vortex Mixer (MIVM) system was developed. In the MIVM, this requirement is less strict, allowing each input to be operated at a separate flow rate[60]. This system utilizes multiple streams to regulate both the level of supersaturation and the ultimate composition of the solvent by adjusting the velocities of the streams. The MIVM facilitates the segregation of reactive constituents prior to amalgamation. The main restriction of formulation screening while using the MIVM is that each run requires a substantial amount of medication, typically in the range of tens of milligrams. Markwalter and Prud'homme developed a smaller version of the MIVM that only needed a minimum of 0.2 mg of a reparative medication for formulation screening[61, 62].

2.4 Nanoparticles

2.4.1 Polymeric Nanoparticles (PNPs)

Polymer-based nanoparticles, with a size ranging from 10 to 1000 nm, have demonstrated their effectiveness as carriers for medicinal medicines. The initial method entails chemically modifying the building units of the amphiphilic BCP. These modifications are often made to add cross-linkable functional groups to one of the polymer blocks or to substitute a specific ligand for the hydrophilic end of the block copolymer. An alternative method to enhance the efficiency of drug delivery devices based on BCPs involves using auxiliary agents such as channel proteins and metal nanoparticles. This method has the appealing advantage of not requiring the block copolymer to be chemically altered because the supplementary agents are just physically contained in the micelles. Using auxiliary agents might improve temporal management by allowing medication release to become pulsatile in response to extrinsic stimuli like magnetic fields or infrared light.[63]. The process of organizing functional BCPs into nanoparticles through self-assembly is valuable for creating delivery

systems that offer exact control over their structure and design. BCP-based nanoparticles have recently been studied for the transportation of pharmaceuticals[64].

The polymer type in flash nanoprecipitation directly affects the supersaturation within the reactor and, consequently the sizes and size distributions. The solubility of polymers can vary based on their structure mainly the difference between the hydrophilic and hydrophobic end. The greater the solubility difference the better the potential to self-assemble into nanoparticles. Also, solubility changes due to chemical structure can cause the hydrophilic part of the block copolymer to be entrapped within the core directly reducing the stability of nanoparticles. Various studies have shown that PEG-PLGA copolymer is one of the best amphiphilic polymers to self-assemble in aqueous solutions into core-shell polymeric structures[49, 65]. Various drugs are included within PEG-PLGA matrices to extend drug circulation durations[66].

2.4.2 Iron Oxide Nanoparticles (IONPs)

Magnetic NPs have garnered significant interest in the field of nanobiotechnology due to their potential uses in biomedicine. Nanoparticles offer significant benefits for transporting drugs within living organisms, thanks to their diminutive dimensions and expansive surface area. Moreover, their magnetic characteristics are crucial for delivering drugs to specific targets. Iron(III) ions are commonly present in the human body, therefore the release of metal is unlikely to result in significant adverse consequences. Maghemite nanoparticles have been extensively studied because of their minimal toxicity at the nanoscale and their favorable magnetic characteristics[67]. The iron oxide nanoparticles that have been extensively researched are magnetite $\gamma\text{-Fe}_2\text{O}_3$ and magnetic Fe_3O_4 . Iron possesses the valuable capacities to undergo reduction and oxidation, to create intricate compounds with diverse biological characteristics, and to engage in electron transfer reactions[68]. The encapsulation of hydrophobic iron oxide nanoparticles (IONPs) using different BCPs(poly(ethylene glycol)-*b*-poly(propylene sulfide) (PEG-PSS), PEG-PLA) has been effectively investigated [69, 70]. Both methods use CIJ geometry to encapsulate IONPs nanoparticles. Some work has also been done on PEG-PLGA block copolymer to coat on IONPs using the modified emulsion evaporation method. The docetaxel DTX-loaded iron oxide nanoparticles (DIONP) exhibited a spherical morphology and a homogeneous size distribution of 220 nm[71].

Thermal activation of Au and γ -Fe₂O₃ particles can be achieved through irradiation with infrared (IR) light or manifestation to an oscillating magnetic field, respectively. Due to the ability of IR light to easily pass through tissue without being absorbed and the lack of unspecific heating caused by exposure to magnetic fields, metal or metal oxide particles are very desirable as auxiliary agents for selectively activating thermosensitive micelles[72, 73].

CHAPTER 3: METHODOLOGY

Materials and Methods

3.1 Materials

The chemicals monomethoxy Polyethylene Glycol (mPEG) with molecular weights of 2000 and 5000, (D,L)-Lactide, Glycolide, Stannous Octoate ($\text{Sn}(\text{Oct})_2$) with a purity of 92%, Oleic Acid (OA) with a technical grade of 90%, and 1-octadecene (ODE) with a technical grade of 90% were obtained from Sigma Aldrich and utilized without additional purification. Iron oleate was synthesized by using the reported method[22] and was used subsequently. The solvents Toluene (anhydrous, 99.8%), Tetrahydrofuran (THF) (analytical, water <0.02%), Dichloromethane (DCM) (anhydrous water < 0.002%), Chloroform (analytical, water<0.01% and chloroform-d as NMR solvent), Diethylether (anhydrous), Hexane (anhydrous), Isopropanol (Technical), and Acetone (Technical) were also acquired from sigma Aldrich. In all the investigations involving polymeric and iron oxide encapsulated nanoparticles, Milli-Q water (MQ) was utilized as an antisolvent.

3.2 Methods of Synthesis

3.2.1 Synthesis of PEG-b-PLGA Copolymer

Two distinct techniques were employed to produce various molecular weights (MWs) of PEG-b-PLGA copolymers. This was achieved by utilizing mPEG with MWs of 2000 and 5000 as macroinitiators.

3.2.1.1 mPEG 2000 MW as a Macroinitiator

To synthesize PEG-PLGA from mPEG 2000 MW as macroinitiator the original work from Jeong, J.H., et al.[52] was adopted. The initial concentrations of monomers were changed to get a lower molecular weight PEG-PLGA copolymer. In a nitrogen environment, specific quantities of D,L-lactide, glycolide, and mPEG were added to a two-neck round bottom flask, which was then heated to 100°C to achieve complete melting. The quantity of mPEG introduced was regulated to modify the MW of the PLGA chain. The compounds D,L-lactide (5.4 g) and glycolide (4.35 g) were mixed with 7.5 g of mPEG. Subsequently, a solution of stannous octoate with a concentration 0.05% (w/w) of reaction mixture was introduced.

Toluene was used as a transportation medium for stannous octoate because of its viscosity and the amount required. The temperature of the reaction mixture was then elevated to 180°C and held steady for a duration of 3 hours. The polymer was obtained by dissolving it in DCM and then precipitating it in ice-cold diethyl ether. The solid was separated by filtration and subsequently desiccated under vacuum.

3.2.1.2 mPEG 5000 MW as a Macroinitiator

The original method from Marinelli, L., et al.[74] was adopted to achieve the desired characteristic. A copolymer consisting of glycolide and D,L-lactide was created using ROP in the molten state, employing mPEG MW 5000 as the initiator and Sn(Oct)₂ as the catalyst.

In summary, D,L-lactide (4.45 g), glycolide (3.58 g), and mPEG (3.09 g) were placed into a round bottom flask. Then, Sn(Oct)₂ (12.5 mg) dissolved in toluene was added. The flask was put under a vacuum to remove the residual solvent (toluene) by opening the bleed valve. The flask was sealed and then placed into an oil bath at a temperature of 180 °C. The melt polymerization continued for a duration of 3 hours under a nitrogen environment. Subsequently, the resulting product was dissolved in chloroform, then precipitated in an excessive amount of diethyl ether, and subjected to vacuum drying for the duration of one night.

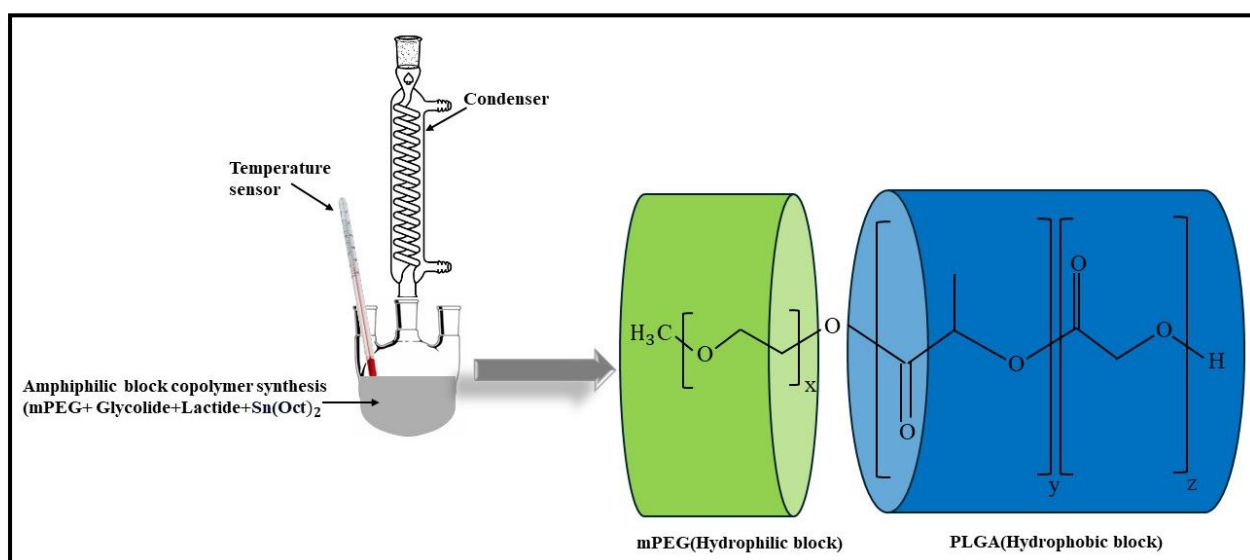


Figure 3.1: Setup for the synthesis of PEGPLGA.

3.2.2 Synthesis of IONPs

Spherical iron oxide nanoparticles (IONPs) were produced by thermal decomposition of a precursor iron oleate at high temperatures in an inert environment of argon following prior work[75]. The reaction temperature was elevated using a temperature controller to achieve accurate control of the heating rate. The production of spherical IONPs entailed combining 1.6 grams of iron oleate, 600 μ l of oleic acid (OA), and 25 ml of ODE in a three-necked glass reactor. The reactor was then positioned on a heating mantle equipped with a cooling water condenser. The reactor's temperature was gradually increased from the initial ambient temperature to 320 $^{\circ}$ C at a rate of 3 $^{\circ}$ C per minute in an argon atmosphere. The reaction was sustained at a temperature of 320 $^{\circ}$ C for a duration of 45 minutes, following which the solution was then cooled to ambient temperature. The NPs were subsequently cleansed with hexane and then separated by precipitation using a combination of isopropanol and hexane. The particles were magnetically isolated and rinsed three times with acetone before being ultimately dispersed in a measured amount of THF[21].

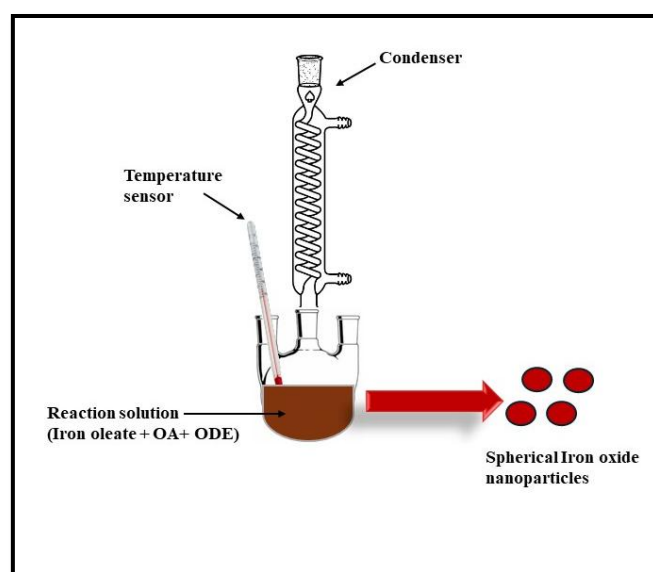


Figure 3.2: Setup for Iron oxide NPs synthesis.

3.2.3 Nanoparticle Formulations using Flash Nano Precipitation

3.2.3.1 Polymeric Nanoparticles

The synthesis of polymeric nanoparticles was adapted from previous works[76, 77]. Using a MIVM system equipped with two inlets, one for the solvent and the other for the antisolvent

were brought to the central mixing component. Different polymer weight percentages in THF were introduced to investigate the variation with particle sizes for both polymers mPEG₂₀₀₀-PLGA and mPEG₅₀₀₀-PLGA. This was done to understand the influence of polymer weight percentages on particle sizes. Six organic solutions were prepared for use in MIVM by dissolving (0.5, 1 and 2 wt%) mPEG₂₀₀₀-PLGA and mPEG₅₀₀₀-PLGA separately in 11 ml of THF. To get the bare PNPs to separate in the multi-inlet vortex mixer (MIVM), the organic solutions were loaded into a 20 ml sterile polypropylene syringe and introduced into the system at a rate of 10 ml/min. The MQ water (antisolvent) was loaded into a 120 ml polypropylene syringe and was adjusted at a flow rate of 100 ml/min. The setup is depicted in Figure 3-1. A 30-second equilibrium period was allocated to the system prior to extracting samples. Three 5 mL samples of nanoparticles were transferred into tiny vials with a 5 s gap between each transfer. Subsequently, the pumps were halted, and the reactor was rinsed by flushing it with 20 mL of THF. Following each batch, THF was also used to clean the interior of the reactor after opening it.

3.2.3.2 PNPs Incorporating IONPs

To harness the benefits of both temporal control provided by polymers and distribution control offered by IONPs, the incorporation of IONPs into polymers was employed to develop optimal carriers for drug administration using the flash nanoprecipitation technique. As far as we know, there is limited research on the inclusion of iron oxide nanoparticles in PEG-b-PLGA copolymer using the flash nanoprecipitation method. Therefore, this study aims to investigate the properties of magnetically directed carriers produced using MIVM. An organic solution

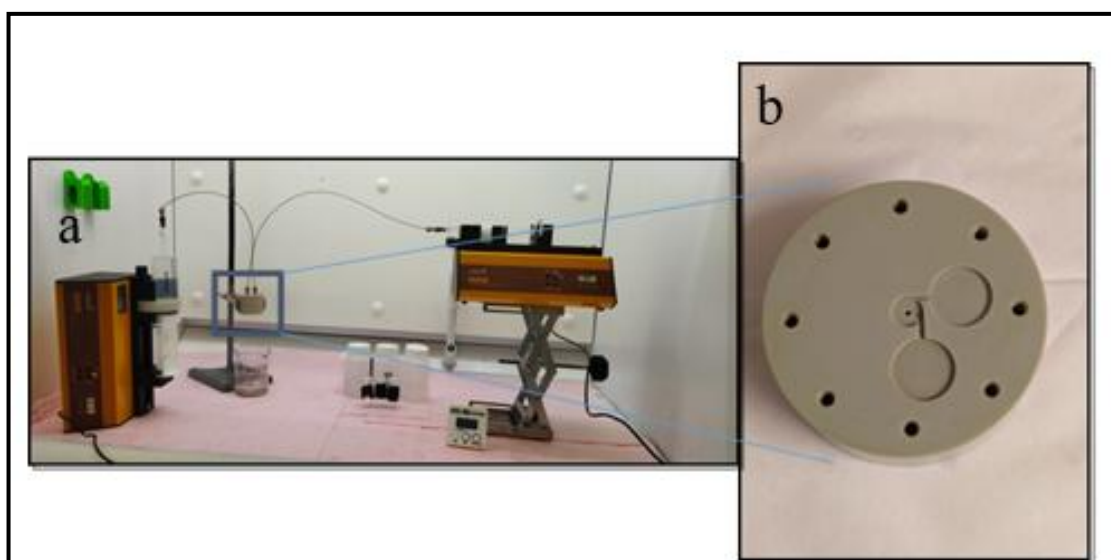


Figure 3.3: (a) FNP setup with syringe pumps and (b) the main reactor for flash nanoprecipitation.

containing 100mg of polymer and 1mg of IONPs was dissolved in 11 ml THF and introduced into the Multi-Inlet Vortex Mixture (MIVM) at the rate of 10 ml/min. Once again, MQ water was utilized as an anti-solvent at a flow rate of 100ml/min, without the presence of any stabilizer. This is because the stability of the nanoparticles was being provided by PEG. This set of tests utilized distinct solutions of PEG₂₀₀₀-PLGA and PEG₅₀₀₀-PLGA.

The coated IONPs were separated from non-coated ones using centrifuge separation at 10000 RPMs. For optimal separation, the collected samples were first transferred to a falcon tube and a magnet was introduced at the bottom for one minute to remove the noncoated ones. As they settled to the bottom, the product sample containing nanoparticles of 13ml was removed from the top. It was cleaned three times, and each time 10 ml was drawn from the falcon tube and 10 ml of MQ water was added along with the sample in the new falcon tube to get the desired results.

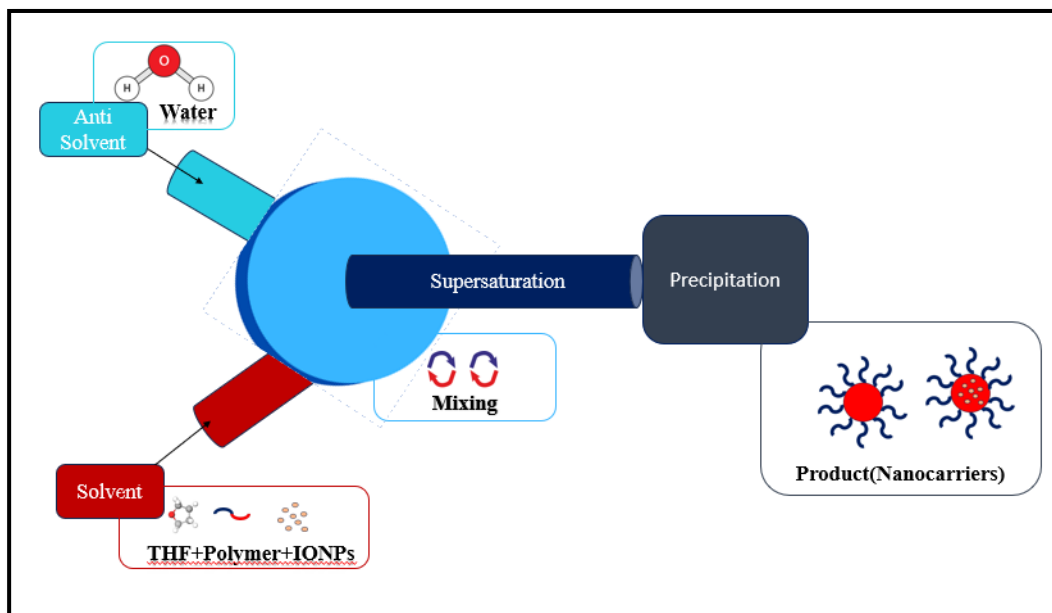


Figure 3.4: Graphics of the FNP Process

3.3 Characterization Techniques

3.3.1 Nuclear Magnetic Resonance

Nuclear magnetic resonance (NMR) spectroscopy is a sophisticated method used for characterizing substances. NMR spectroscopy is employed to ascertain the atomic-level molecular arrangement of a specimen, relying on the rotation of the nucleus that generates a

magnetic field[78]. In addition to analyzing the molecular structure, NMR spectroscopy offers the capability to ascertain phase transitions, changes in conformation and configuration, solubility, and diffusion potential. The nuclei sample is positioned within the magnetic field and subsequently stimulated into nuclear magnetic resonance through the application of radio waves. In the NMR 600Mhz Bruker Avance instrument, a signal is produced and subsequently detected by a radio frequency receiver. An atom is surrounded by an intermolecular magnetic field that causes the resonance frequency to change. This can offer the structural and compositional characteristics of the molecules. Due to variations in the chemical environment of each molecule, their resonance frequencies will likewise differ. This enables the acquisition of distinct NMR spectra for various compounds. NMR can be utilized to assess stereoisomerism, sequence- and structural isomerism, and analyze the copolymer composition.

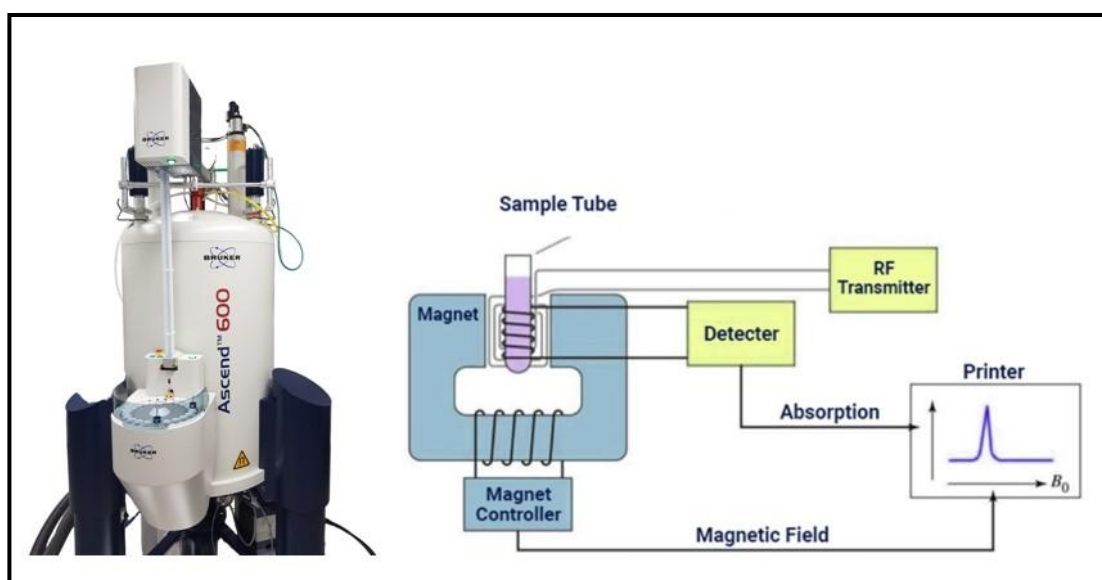


Figure 3.5: Working of NMR Spectroscopy

¹H-NMR spectroscopy is performed to verify the successful production of the copolymer. The ¹H-NMR spectra of copolymers reveal distinct resonance spectra compared to the monomers when exposed to diverse conditions. The displacement of the peak resulting from the copolymers' synthesis is evident in the NMR spectra, providing additional support for the conducted research. ¹H-NMR was used to determine the molar ratio of lactide to glycolide in the PEG-PLGA block copolymer. The subsequent formulas were used to determine the molar percentage of contributing units, specifically lactic acid (%L) and glycolic acid (%G).

$$I_G = I_{4.8-4.9/2}$$

$$I_L = (I_{1.5/3} + I_{5.1-5.2})/2$$

$$\% L = (I_L / (I_L + I_G)) \times 100$$

$$\% G = (I_G / (I_L + I_G)) \times 100$$

where I_G and I_L are the peak integrals per proton for each monomer unit[74].

3.3.2 Fourier Transform Infrared Spectroscopy (ATR-FTIR)

The functional groups and interfacial interactions were determined using Attenuated Total Reflectance Fourier Transform Infrared (ATR-FTIR) analysis, namely using the BRUKER Vex 70 instrument. The primary goals of FTIR are to recognize the distinctive functional groups present in each monomer that contribute to the features of the copolymer and iron oxide. The study was conducted within the region of $4000-400 \text{ cm}^{-1}$, with a scanning frequency of 100 and a resolution of 4 cm^{-1} . The polymer and nanoparticles were subjected to FTIR analysis to ascertain any alterations in terms of the chemical functionalities.

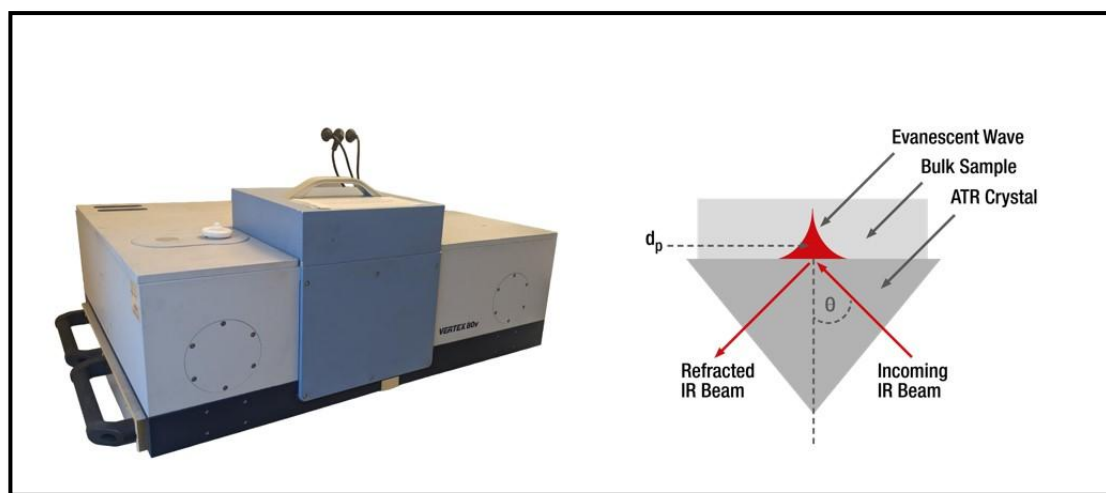


Figure 3.6: Working Mechanism of ATR-FTIR[79]

The operational mechanism of the ATR-FTIR spectrometer involves the transmission of infrared light through a crystal which, at the interface between the crystal and the sample,

experiences complete internal reflection. The reflected beam is sent towards the FTIR detector. During internal reflection, a portion of the infrared light is also transmitted to the sample and is absorbed by it. The wave in question is commonly known as the evanescent wave. The penetration depth of this wave into the sample is determined by the disparity between the refractive indices of the ATR crystal and the sample. Various ATR sensors made of different materials are utilized for different types of samples[80, 81].

3.3.3 X-ray Crystallography (XRD)

The instrument used is the Bruker D8 A25 DaVinci X-ray Diffraction (XRD) with $\text{CuK}\alpha$ radiation. The LynxEye™ SuperSpeed Detector was utilized to analyze the crystalline structure of IONPs. X-ray diffraction, sometimes known as XRD, is a technique used to analyze the arrangement of atoms in crystalline substances. X-ray diffraction (XRD) operates by exposing a sample to an X-ray beam, causing the atoms in the sample to scatter the X-rays in different directions. The spatial configuration of atoms within the material can be ascertained by quantifying and examining the X-ray diffraction pattern. The X-ray source operates at a voltage of 40Kv and a current of 40mA. The $\text{CuK}\alpha$ radiation emitted by the source has a wavelength of $\lambda = 1.5406\text{\AA}$. XRD aids in the determination of crystallinity and distinguishes between crystalline and amorphous states[82].

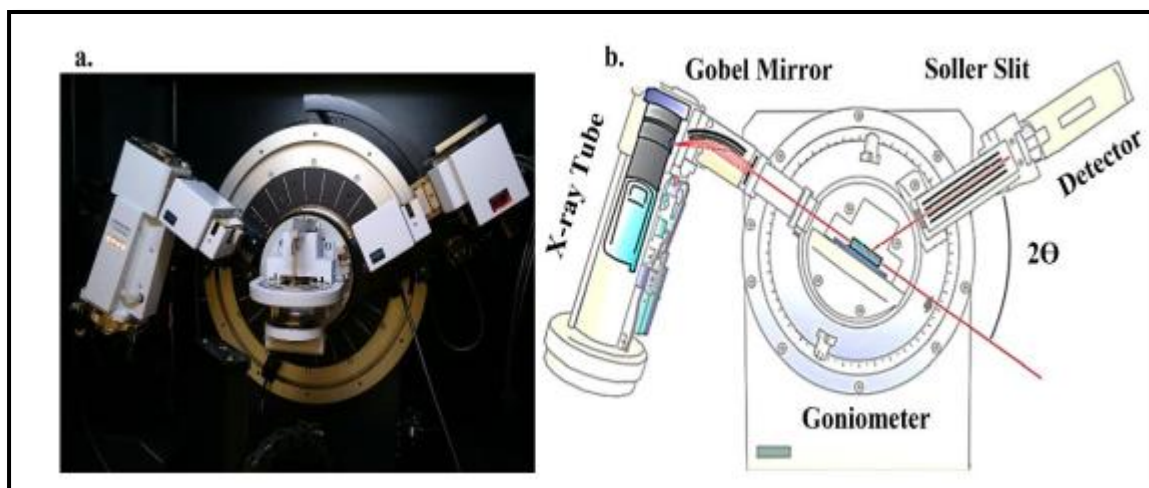


Figure 3.7:(a) Bruker D8 A25 DaVinci XRD (b) Schematic showing the main components of XRD

3.3.4 *Scanning Transmission Electron Microscope (S(T)EM)*

S(T)EM is a method that integrates the fundamental principles of Scanning Electron Microscope (SEM) and Transmission Electron Microscope (TEM). Scanning (Transmission) Electron Microscopy (STEM) is a very effective imaging method employed in the field of materials science and engineering to investigate the nanoscale structure and composition of materials. STEM imaging necessitates the use of extremely thin samples, where a concentrated beam of high-energy electrons is directed onto the sample in a raster pattern. In S(T)EM, two main categories of signals can be observed: transmitted electrons and scattered electrons. The transmitted electrons traverse the atom without any interaction and are utilized to generate a high-resolution depiction of the internal composition of materials. The electron beam's interaction with the atoms in the sample results in the scattering or absorption of some electrons, which is determined by the atomic number and thickness of the atoms. The electrons that are dispersed and propagated are detected by a sequence of detectors situated both above and below the sample.

The detectors' data is subsequently processed to provide an image of the sample that exhibits exceptional resolution and contrast, therefore exposing the intricate atomic composition of the material. The detectors found in the (S(T)EM) are specialized and include bright-field detectors, dark-field detectors, and high-angle annular dark-field detectors. These detectors provide the generation of a variety of pictures and the analysis of materials. Analyzed utilizing scanning transmission electron microscopy (STEM), the produced bare polymeric nanoparticles (PNPs), iron oxide nanoparticles (IONPs), and PNPs combined with IONPs were examined.

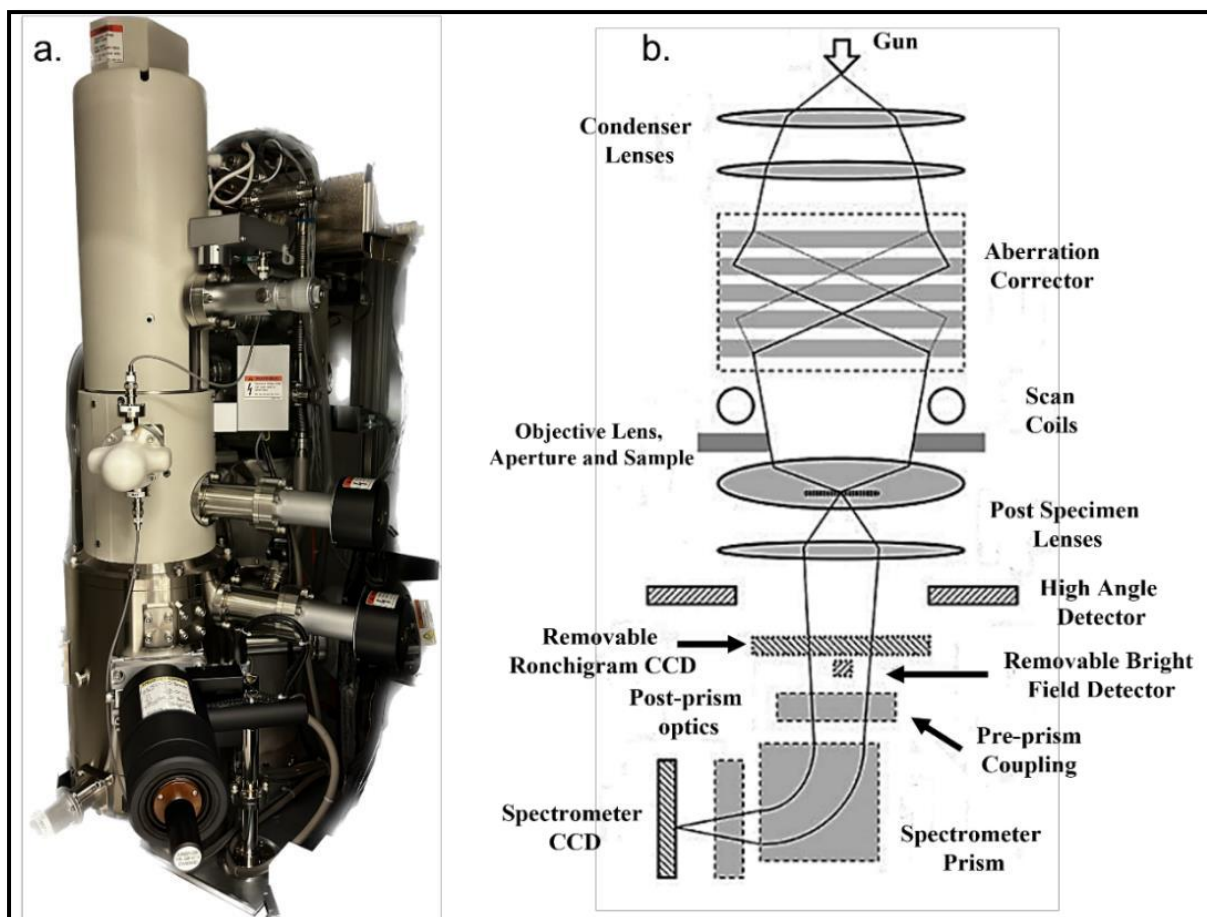


Figure 3.8: (a)High resolution S(T)EM Components (b) Schematic showing the main components of S(T)EM [83]

3.3.5 *Dynamic Light Scattering (DLS)*

Dynamic Light Scattering (DLS) enables precise characterization of particle sizes within the nanometer scale. The device functions based on the idea of Brownian motion, where a laser source illuminates a sample, causing the particles to scatter light due to their motion, resulting in a scattering signal. A detector detects this signal, and after analyzing it with a computer, we obtain the hydrodynamic size of the particles. The particles in the sample initiate Brownian motion upon exposure to light. The particles in the sample exhibit varying velocities based on their respective sizes, with smaller particles exhibiting higher velocity compared to bigger particles. The mechanics of particle movement determine their size. The distribution is derived by utilizing the ratio between the quantities of large and small particles detected. The study utilized the Anton Paar Litesizer to determine the size, distribution, and Zeta potential (ZP) of

particles[84]. The nanoparticles generated by FNP were immediately examined using the Dynamic Light Scattering DLS (Anton Paar Litesizer 500) instrument. The suspension of FNP NPs (800 μ L) was placed in a capped polystyrene disposable cuvette. The measurement of the hydrodynamic size was initiated at a temperature of 25 °C, with a maximum of 60 runs at 10-second intervals, using the automatic setting. The zeta potential of the nanoparticle's solution was determined using an OMEGA®28 cuvette.



Figure 3.9: Anton Paar LiteSizer 500

3.3.6 Gel Permeation Chromatograph (GPC)

GPC, or size exclusion chromatography (SEC), is a liquid chromatography technique used to separate polymer samples depending on the size, specifically the molecular hydrodynamic volume, of distinct molecules. Figure 13 illustrates that the separation process takes place within interconnected columns containing stationary phase materials, such as polystyrene and silica gel. The stationary phase consists of minute particles that possess many holes of varying diameters. Upon dissolution of the polymer sample in the solvent, it is hypothesized that the polymer chains get intertwined from spherical structures of varying molecular dimensions. As the mobile phase flows through the columns, the bigger spherical units (highlighted in red) are prevented from passing through the smaller pores in the stationary phase. This is due to the size exclusion effect. Consequently, molecules of significant size are rapidly separated and their elution period, or retention time, is reduced. By contrast, tiny molecules (shown by the color blue) pass through a wider network of microscopic pores, resulting in a longer elution time or retention time. According to this approach, a polymer sample can be divided into molecules of varying sizes, which are then measured as varied elution times. GPC has been

used to determine the MWs and polydispersity of polymers using THF as a solvent in our case. A 3mg sample of polymer was dissolved in 1 mL of tetrahydrofuran (THF). The material underwent syringe filtration and was thereafter placed into a 1 mL HPLC vial, and the elution rate was 1 ml/min. The Agilent 1260 Infinity II was utilized in conjunction with the refractive index detector. The molecular weight was automatically calculated using the Agilent GPC/SEC system. Software equipped with a calibration curve based on polystyrene.

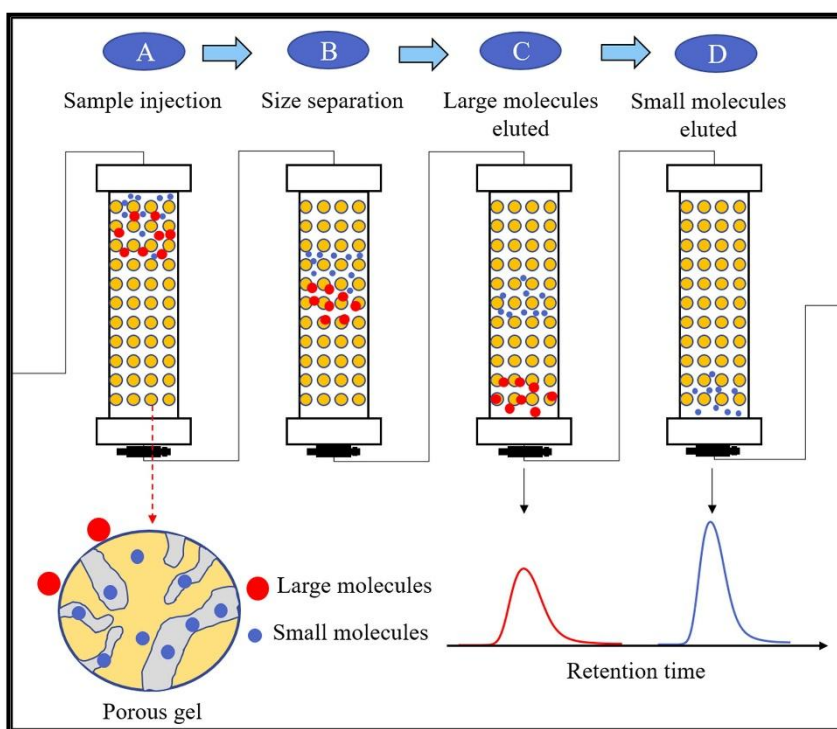


Figure 3.10: Schematic diagram of the separation principle of gel permeation chromatography (GPC)

[85]

CHAPTER 4: RESULTS AND DISCUSSION

4.1 Characterization of Polymers

The PEG-b-PLGA copolymer was synthesized via ROP using Glycolide, (D,L) Lactide, and mPEG as an initiator. The conformation of copolymer synthesis is mostly analyzed based on the features of the monomers that contribute to the copolymer. The section below examines and analyzes PEG-PLGA block copolymer with different MWs using NMR, GPC, and FTIR techniques. To verify the presence of inherent features in the copolymers PEG₂₀₀₀-PLGA and PEG₅₀₀₀-PLGA. The synthesised copolymers have lower molecular weights compared to the work we used as a reference, due to the use of differing ratios of monomers.

4.1.1 Nuclear Magnetic Resonance (NMR)

The copolymer analysis is obtained by examining the proton nuclear magnetic resonance (¹H NMR) spectra of both PEG₂₀₀₀-PLGA and PEG₅₀₀₀-PLGA. The copolymer was subjected to compositional investigation using H-NMR spectroscopy, with chloroform-d used as the solvent. The synthesis process is assessed by quantifying the ratio of resonance integration of PEG blocks at 3.64 ppm (OCH₂CH₂), LA at 1.58 ppm (CH₃), and GA at 4.80 ppm (CH₂)[52]. The presence of minor vibrations in the methylene protons (**b**) at the connection site between the PEG and PLGA blocks suggests that the polymerization process was successful and maintained a high level of functional accuracy[86].

The NMR spectra depicted in Figure 4-1 provide additional evidence supporting the fabrication of a block copolymer with a nearly equal ratio of glycolide to lactide. Generally, a higher content of PGA typically results in faster deterioration rates as compared to when lactide content increases[87]. However, there is an exception when the ratio of PGA to PLA is 50:50, it shows the fastest degradation[88]. The molecular structure of the copolymer gives rise to distinct peaks that correspond to different proton environments.

Table 4.1: Molar ratio of glycolide to lactide

Polymer	Glycolide %	Lactide%
PEG ₂₀₀₀ -PLGA	51	49
PEG ₅₀₀₀ -PLGA	51	49

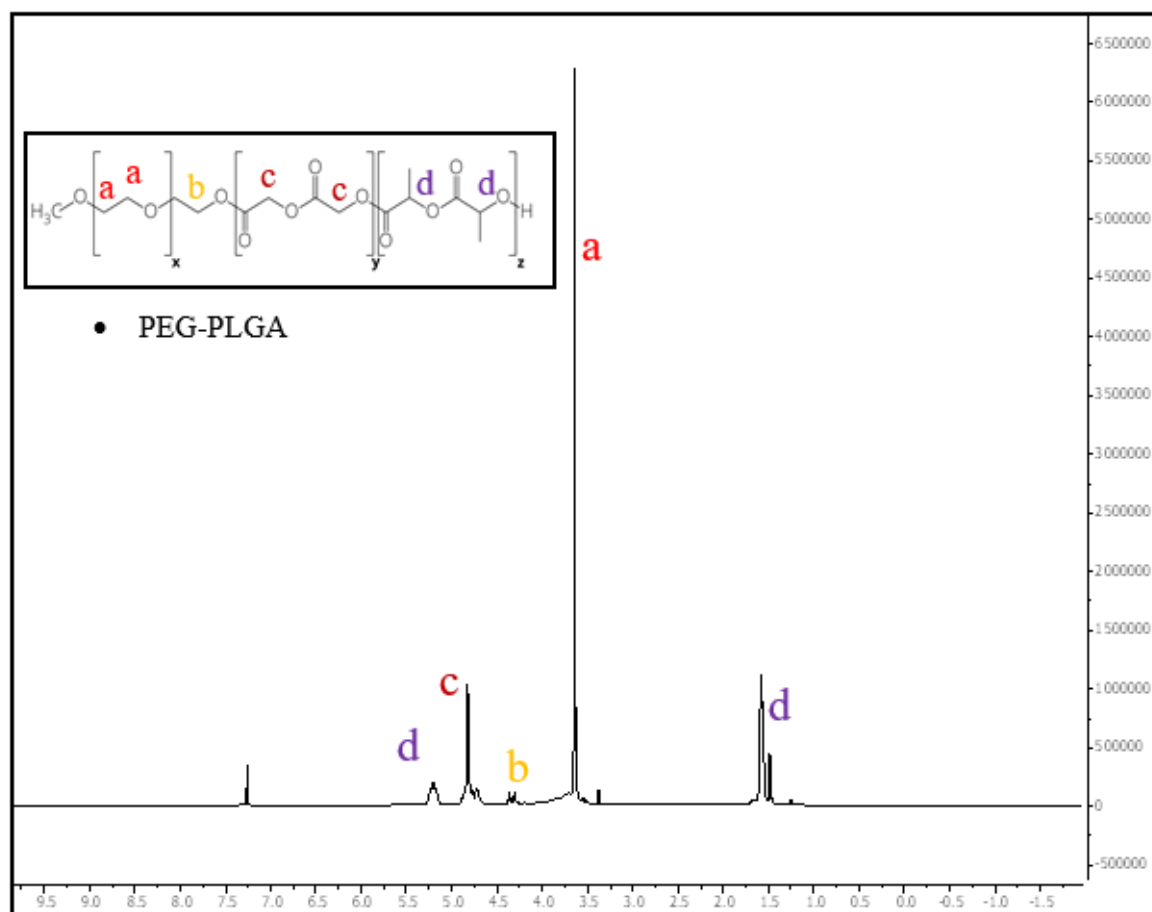


Figure 4.1: Proton nuclear magnetic resonance (¹H NMR) spectra of mPEG-b-PLGA

4.1.2 Gel Permeation Chromatograph

The weight average molecular weight (M_w) and polydispersity (PDI) of both polymers were decided using GPC analysis shown in Table 4.2. The PDI (Polydispersity Index) data indicated that PEG₂₀₀₀-PLGA had a narrower molecular weight distribution of 1.39, whereas PEG₅₀₀₀-PLGA had a higher value of 1.69 because of different initial monomer concentrations. The produced polymer had a composition (MW) that closely resembled the molecular weights of

the monomer inputs such as PEG (2000 and 5000) while the remaining MW percentage must be from lactide and glycolide monomers.

Table 4.2: Molecular weights and polydispersity measured through GPC

Polymer	Mn (g/mol)	Mw (g/mol)	PDI
PEG ₂₀₀₀ -PLGA	3570	5178	1.45
PEG ₅₀₀₀ -PLGA	6563	10631	1.62

4.1.3 Fourier Transform Infrared Spectroscopy (FTIR)

The FTIR spectra of the copolymer, as depicted in Fig. 4-2, validate the chemical composition of the copolymer about the monomer. The bands observed at 3010 and 2955 cm^{-1} correspond to the stretching of the C–H bonds in the CH_3 group, while the band at 2885 cm^{-1} corresponds to the stretching of the C–H bonds in the CH_2 group. The C=O stretch is associated with a prominent peak at 1750 cm^{-1} and 1465 cm^{-1} is attributed to H–C–H bending. The absorption observed at the wavenumbers of 1186–1089.6 cm^{-1} is attributed to the stretching of the carbon-oxygen (C–O) bond[89]. FTIR spectra of PEG-PLGA copolymer with different MW initiators

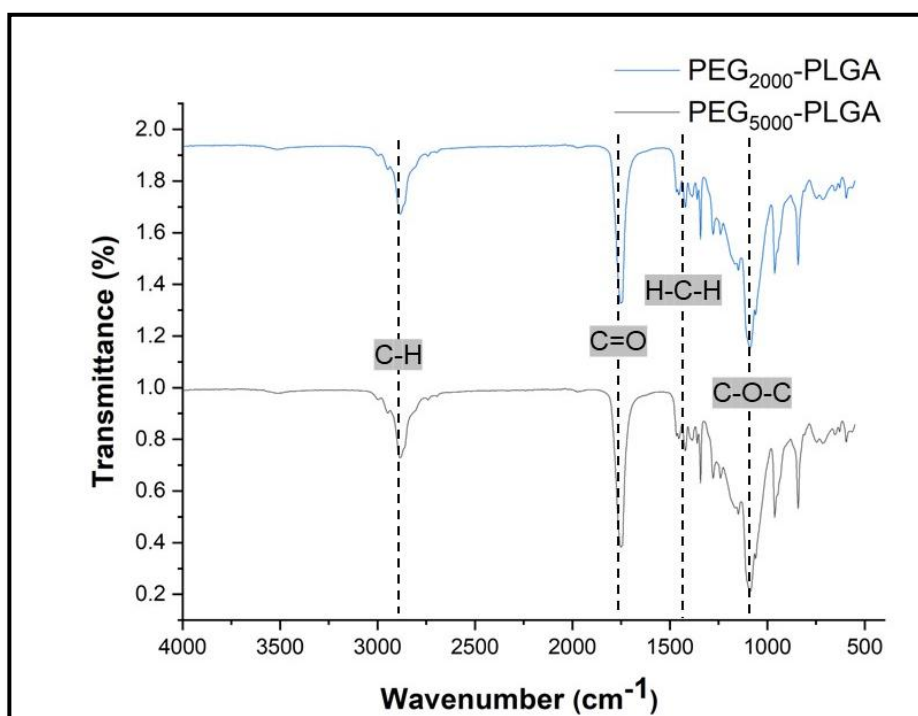


Figure 4.2: FTIR spectra of PEG-PLGA copolymer with different MW mPEG initiators.

4.2 Characterization of Iron Oxide Nanoparticles

4.2.1 X-ray diffraction spectroscopy

The iron oxide nanoparticles were synthesized as previously described in Chapter 3 section 3.2.2. The crystal structure and phase analysis of the synthesized nanospheres were examined by XRD characterization. The XRD peaks exhibit a strong resemblance to the magnetite Powder Diffraction File (PDF) card no. 88-0315, from the International Centre for Diffraction Data (ICDD). Upon initial examination of the patterns, it is evident that there is significant peak broadening, suggesting that the material possesses a remarkably diminutive crystallite size. Furthermore, the coexistence of a blend of wide and slightly more defined peaks signifies the existence of anisotropic size broadening. The varying widths of the observed diffraction peaks can be explained by the presence of varied crystallite sizes along different crystallographic directions. The diffraction peak matches with the XRD analysis by Zhen, G., et al. for the synthesis of spherical IONPs[90]. . The data as shown in Fig. 4-3 highlights diffraction peaks at $2\theta = 30.08^\circ$, 35.44° , 43.19° , 53.51° , 57.01° , 62.86° , and 74.12° , which can be indexed to the (220), (311), (400), (422), (511), (440) and (533) planes of Fe_3O_4 respectively[91].

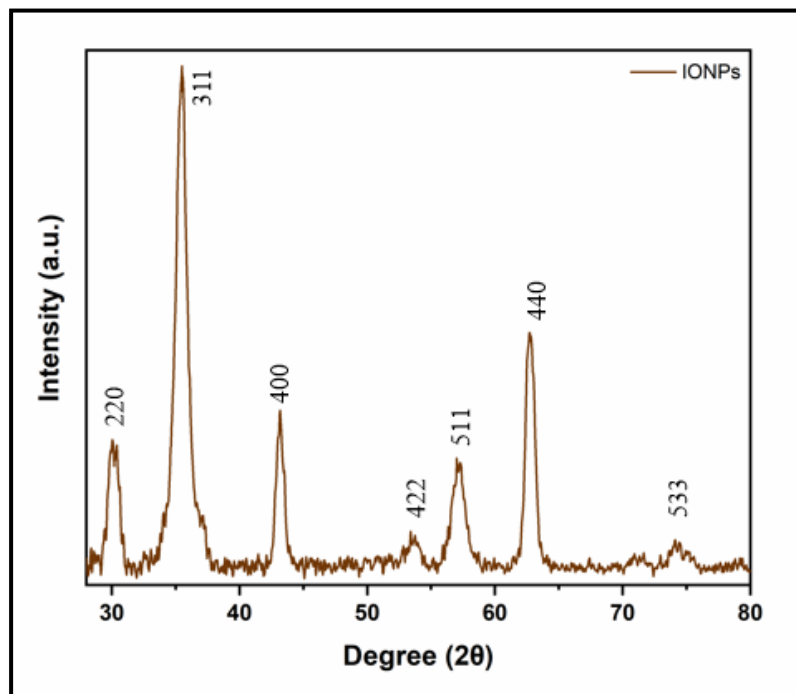


Figure 4.3: X-rays Diffraction Spectroscopy of IONPs

4.2.2 Transmission Electron Microscopy and Vibrating Sample Magnetometer (VSM)

Transmission Electron Microscopy STEM is a powerful tool used for the topographical analysis of materials. It provides in-depth information about structure, and crystallographic properties. The synthesized IONPs were analyzed in TEM to get information about their sizes and shapes. Figure 4-4 confirms the synthesis of spherical morphology with an average diameter of 15 ± 2 nm as expected from the experiments.

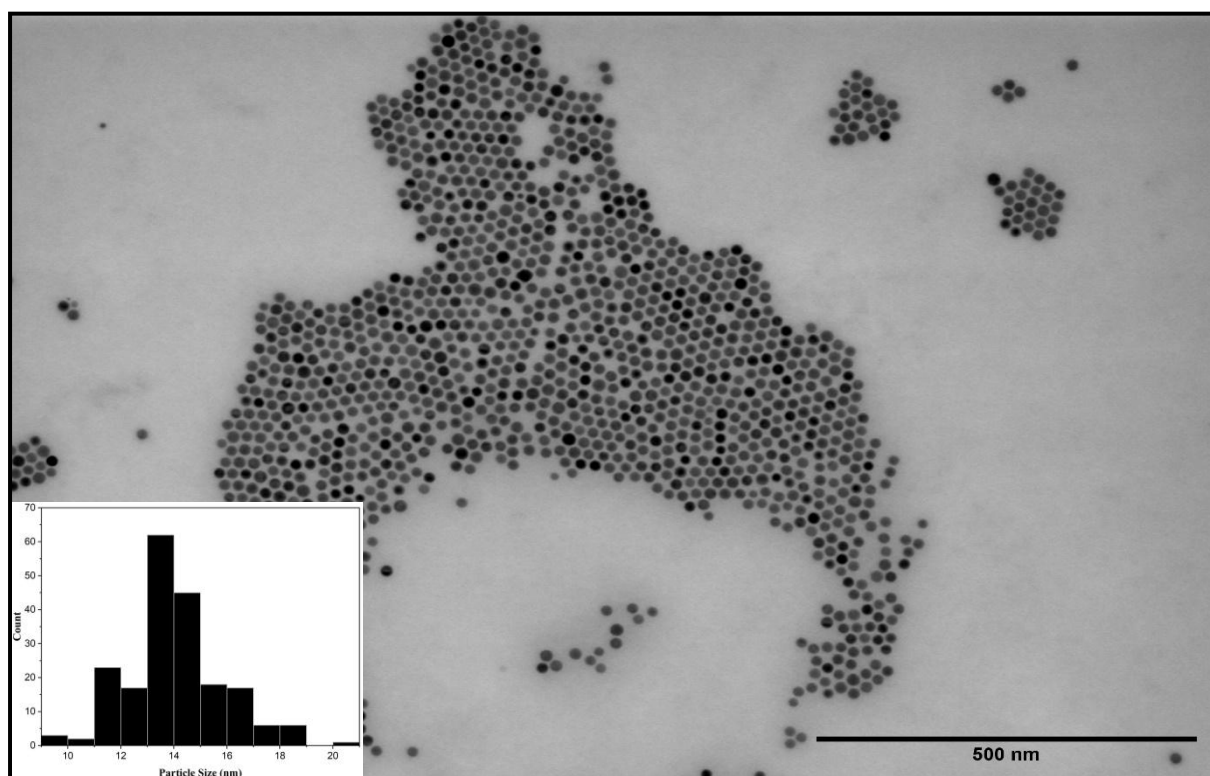


Figure 4.4: TEM image of Iron Oxide Nanoparticles with uniform size distribution.

The magnetic characteristics of the fabricated IONP powder were analyzed using a VSM at ambient temperature which confirmed the superparamagnetic character of the particles as illustrated by the M vs. H curve Figure 4-5. The slight hysteresis is due to the number of particles utilized for characterization and the instrument's reduced precision at low fields. The curve formed shows superparamagnetic however when normalized for mass, the magnetization is smaller, 23.32 emu/g, than what has been previously documented in the literature. This could be explained by the presence of unreacted precursor in the finished sample, which would

significantly increase the iron content but not the sample's magnetic characteristics[92]. By further optimizing reaction parameters and purification methods, these results can be enhanced by achieving a greater reaction yield.

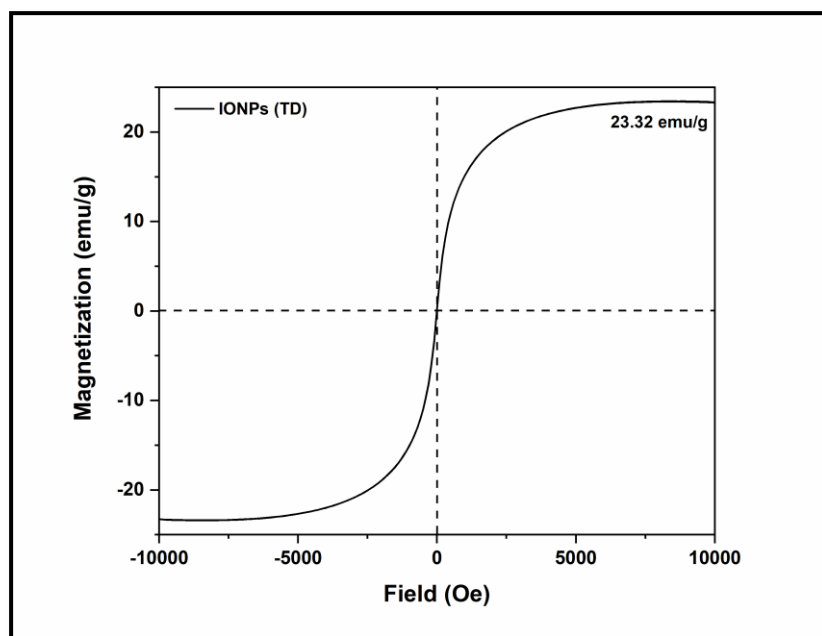


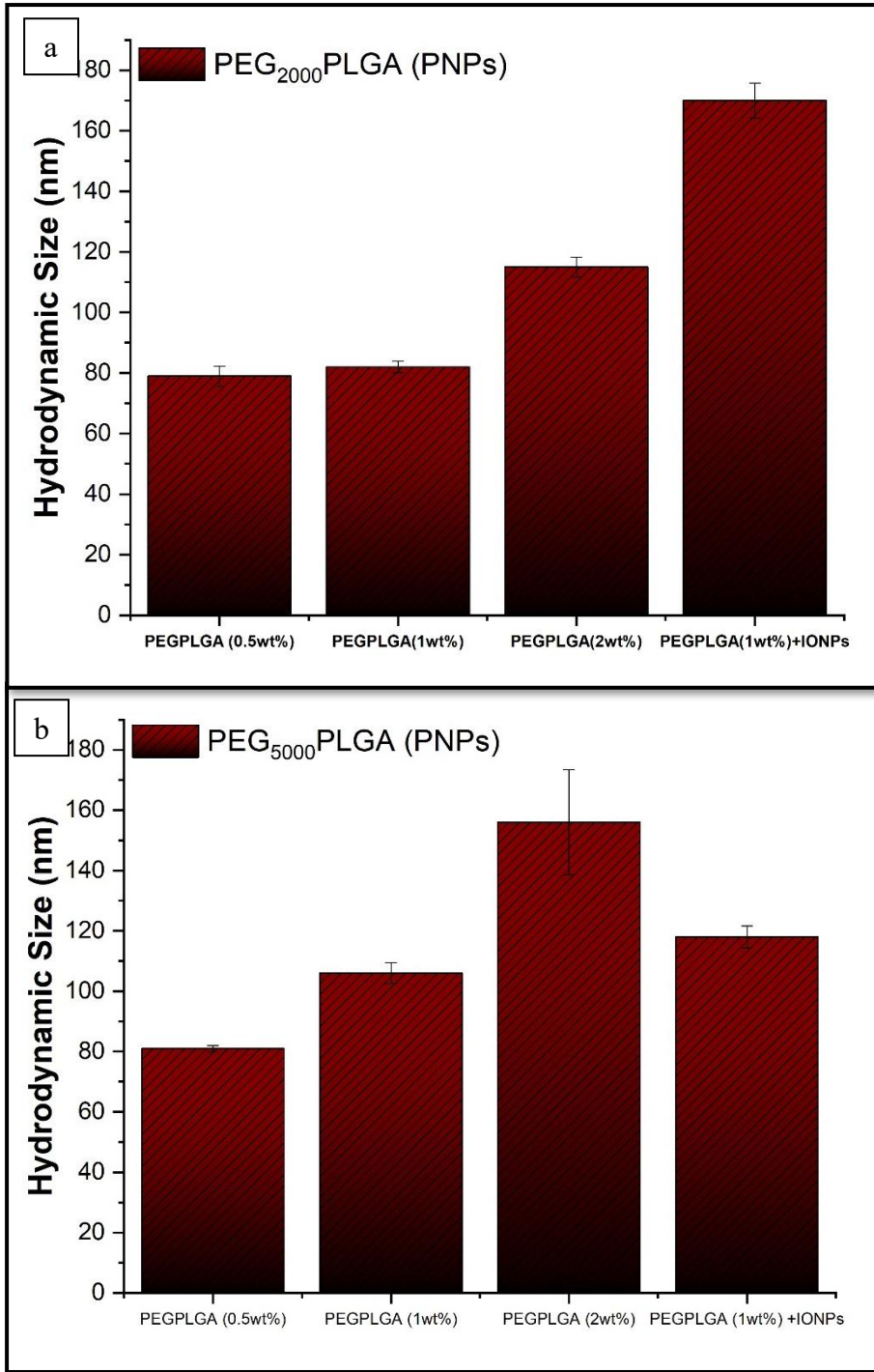
Figure 4.5: Characterization of IONPs against applied field

4.3 Nanoparticles Characterization Synthesized using MIVM

4.3.1 Sizes of Nanoparticles: Bare PNPs and PNPs incorporating IONPs

Following the work by Pustulka, K.M.[49] to study the variation of polymer concentration. For the bare polymeric nanoparticles, 0.5, 1, and 2 weight percentages of polymers were added in THF, and for PNPs encapsulating IONPs, 1 wt % polymer was added along with 1mg IONPs in THF and was synthesized using MIVM as explained in chapter 3 section 3.2. An augmentation in the hydrophobic segment frequently leads to an enlargement in the particle size[93]. This is shown in Figure 4-6, as the weight percentage of polymers increases so do the sizes of nanoparticles. The increase in sizes is more evident in PEG₅₀₀₀-PLGA as compared to PEG₂₀₀₀-PLGA. Lower molecular weight PEG₂₀₀₀-PLGA is more soluble in THF, resulting in smaller but more monodisperse particles which are sterically stable in the final solution. The size dependencies on polymer concentration and molecular weights may be elucidated by examining polymer chain density in the solvent and the impact of polymer concentration on

viscosity. Due to the higher concentration of polymer chains in the solvent, more polymer chains diffuse into the aqueous phase, leading to the aggregation and formation of bigger nanoparticles. [94]. PNPs that incorporate IONPs have also been analyzed and their sizes were determined. For bare PEG₂₀₀₀-PLGA NPs, the sizes were 82nm, but when IONPs were incorporated, the sizes increased to 170nm, resulting in uneven associations. On the other hand, for PEG₅₀₀₀-PLGA, the particle size does not change significantly. The bare particle size was 106nm, and when IONPs were incorporated, it increased to 118nm for PNPs giving stable more uniform structures In both instances, the total size of nanoparticles grew[22].



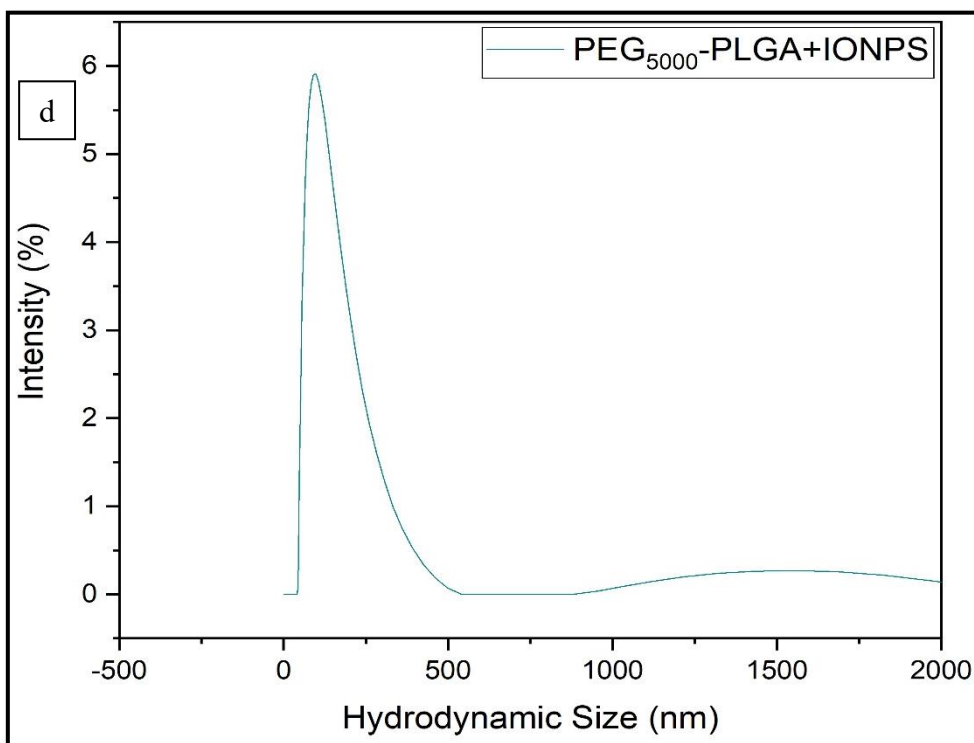
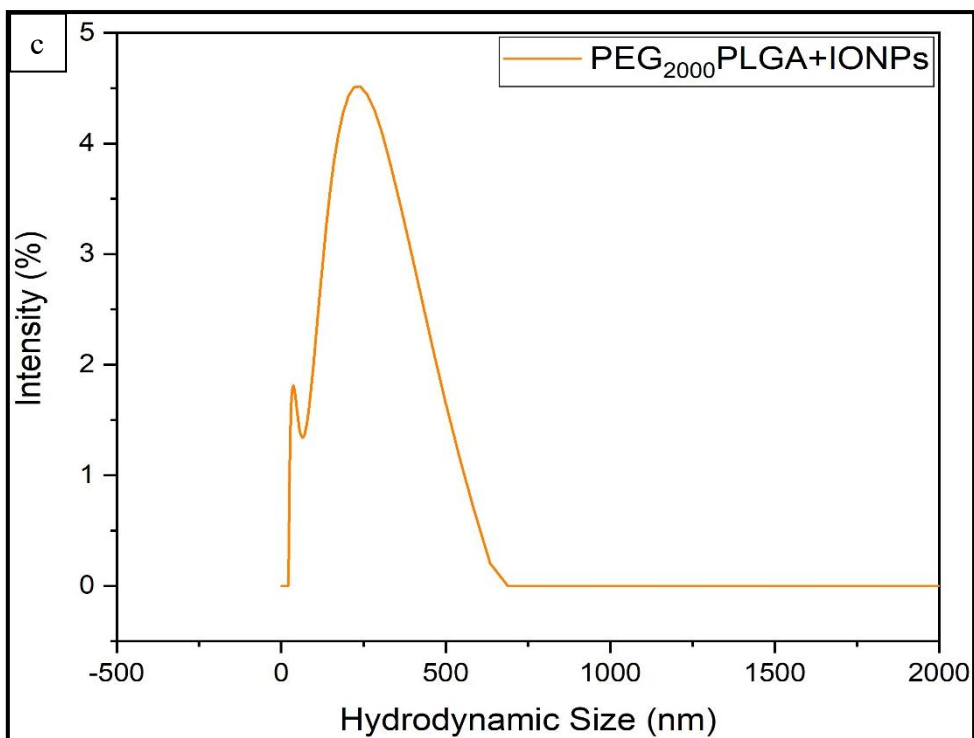


Figure 4.6: Sizes of Bare PNPS (0.5,1 and 2 wt.%) vs. PNPs combined with IONPs (a,b) and Distribution (intensity%) plots from DLS data corresponding to the IONPs coated polymer data (c, d)

4.3.1.1 Stability of Nanoparticles

Nanoparticle stability pertains to the capacity of nanoparticles to sustain their dimensions, configuration, and distribution without aggregating or experiencing chemical alterations over a period of time. It is impacted by various elements including surface charge, pH, temperature, and the existence of stabilising agents. During the examination of bare nanoparticles, there were deliberations on their stability, which is influenced by the hydrophobic and hydrophilic components of the block copolymer (BCP) as well as the method of synthesis. Previous works have prepared PNPs of PEG-b-PLGA using FNP which were stable for 10 days [49] and there are a lot of studies about the stability of non-degradable PNPs[95, 96]. In this study, we analyze the properties of degradable PEG-b-PLGA, which was synthesized using FNP with the assistance of MIVM. PEG polymer coatings can provide a physical barrier, keeping nanoparticles apart and acting as a stabilizing agent. Nanoparticle suspensions should maintain a restricted size distribution for extended periods, ranging from days to weeks or even months. We employ (DLS) to ascertain these PEG attributes. Our findings confirm that nanoparticles didn't form clusters exceeding ten days under ambient conditions, supporting the hypothesis that a lower amount of PEG is trapped in the core, providing stability through the shell as shown in Figure 4-7.

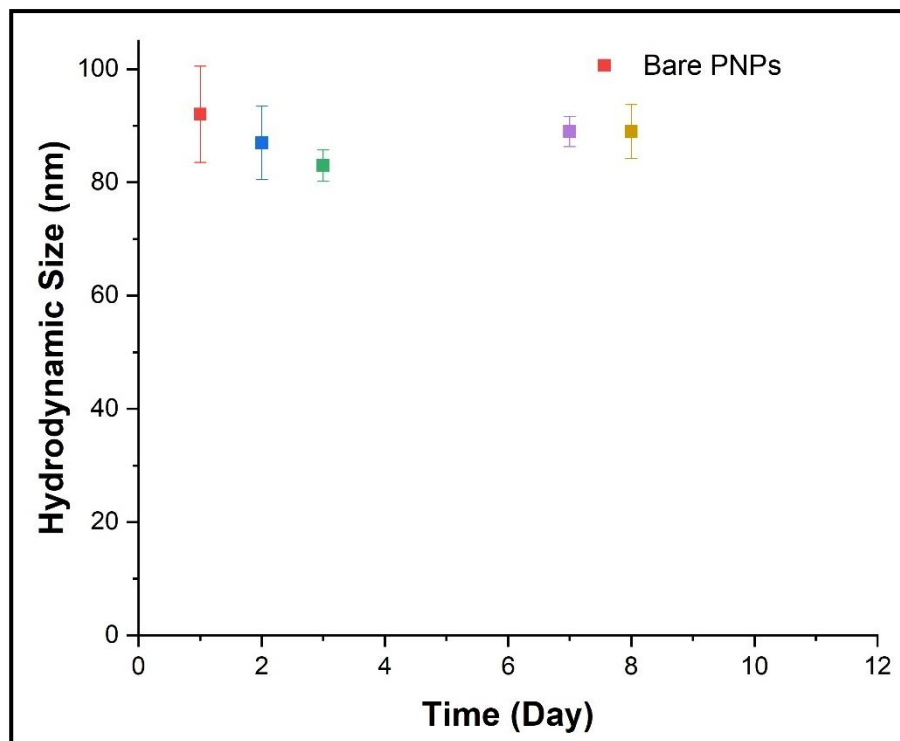


Figure 4.7:Stability of PNPs characterized by DLS

4.3.1.2 pH and Surface Charge Impacts on Nanoparticles

After the production of nanoparticles, it is important to consider their colloidal stability with environmental factors such as pH and surface charge. In amphiphilic block copolymer (BCP) systems, whether other polymers are present, stabilization occurs due to the self-assembly of

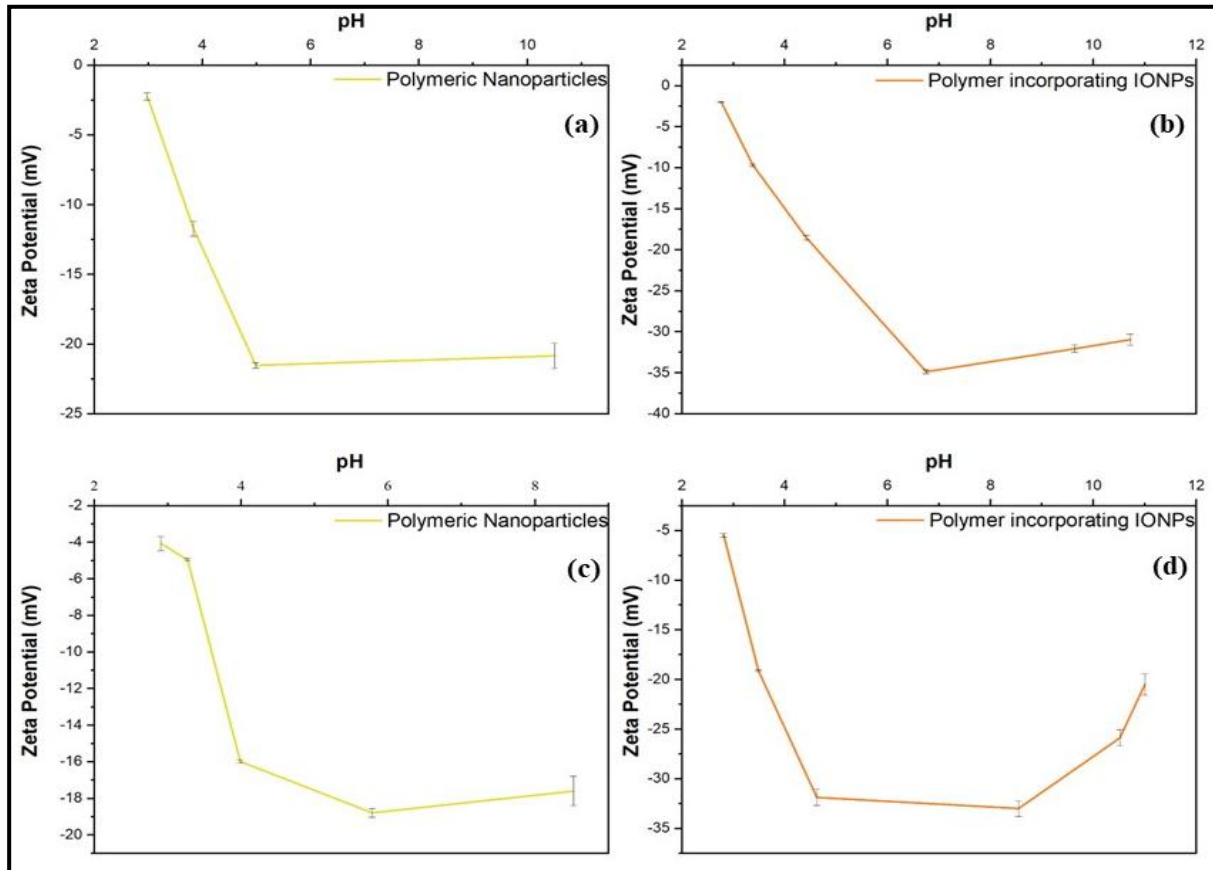


Figure 4.8: Comparison of colloidal stabilities for both (a,b) PEG₂₀₀₀PLGA and (c,d) PEG₅₀₀₀PLGA: Bare PNPs vs. PNPs incorporating IONPs

BCPs when the solvent quality changes. The core-corona structure of a BCP NP is confined kinetically, meaning it is unable to easily undergo unimer exchange and fusion due to a significant energy barrier. This barrier effectively slows down the aggregation processes[97]. In this study, we aimed to demonstrate the intrinsic stability of the synthesized nanoparticles with varying external factors of pH and surface charge open. Additionally, the inclusion of IONPs proved advantageous, as it allowed the particles to function effectively as drug delivery carriers across various pH settings. Figure 4-8 shows the variation of zeta potential with pH for both types of nanoparticles. Particles exhibiting significantly negative or positive zeta potential values tend to reject one other. It can also be seen that the addition of IONPs to polymer gave zeta potential values with higher magnitude, so they contribute positively toward the dispersion

of particles. The aggregation potential will be lowest where the particles have shown highly negative zeta potential values which mostly correspond to a pH range of 5-8. In that range, particles will have less of an affinity to aggregate while maintaining their form and structural integrity.

4.3.2 Fourier Transform Infrared Spectroscopy:

Figure 4-9 compares the FTIR of PNPs with IONPs incorporated PNPs. The inherent bands of polymer have already been discussed in this chapter and they remained the same with varying intensities for polymeric nanoparticles. However, when IONPs were added to the polymer it caused a shift in the parent polymer bands. A slight shift was observed for C=O stretch from 1755 to 1747 cm^{-1} . A dominated stretch associated with Fe-O bond appears at 597 cm^{-1} which shows a shift from the inherent Fe_3O_4 band at 574 cm^{-1} [21]. These shifts without focusing on the IONP encapsulation, showcase the bonding between polymer and IONPs

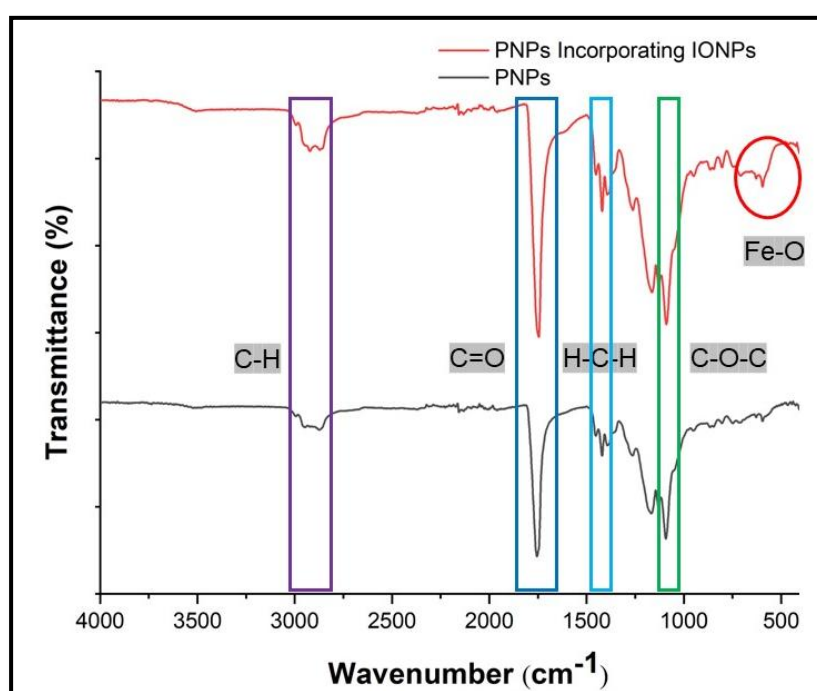


Figure 4.9: FTIR spectrums comparing bare PNPs vs PNPs-IONPs

4.3.3 Scanning (Transmission) Electron Microscopy:

The most effective technique for topographical analysis is S(T)EM. The S(T)EM is a hybrid imaging technique that combines the capabilities of both TEM (Transmission Electron Microscopy) and SEM (Scanning Electron Microscopy). The produced PNPs, both with and

without included IONPs, were examined using STEM in SEM mode to observe their structure. Figure 4-3 confirms the presence of synthesized PNPs with a distinct three-dimensional architecture and a spherical size distribution. Fig. 4-10 illustrates the concentrated regions created by exposed PNPs of both PEG₂₀₀₀PLGA and PEG₅₀₀₀PLGA polymers. The dimensions of PNPs are also somewhat smaller than those reported using DLS. It is easier to understand these results if one takes into account the variations in methods. The DLS approach considers the hydrodynamic diameter of particles in suspension, while TEM pictures consider the gyration radius of dried particles.

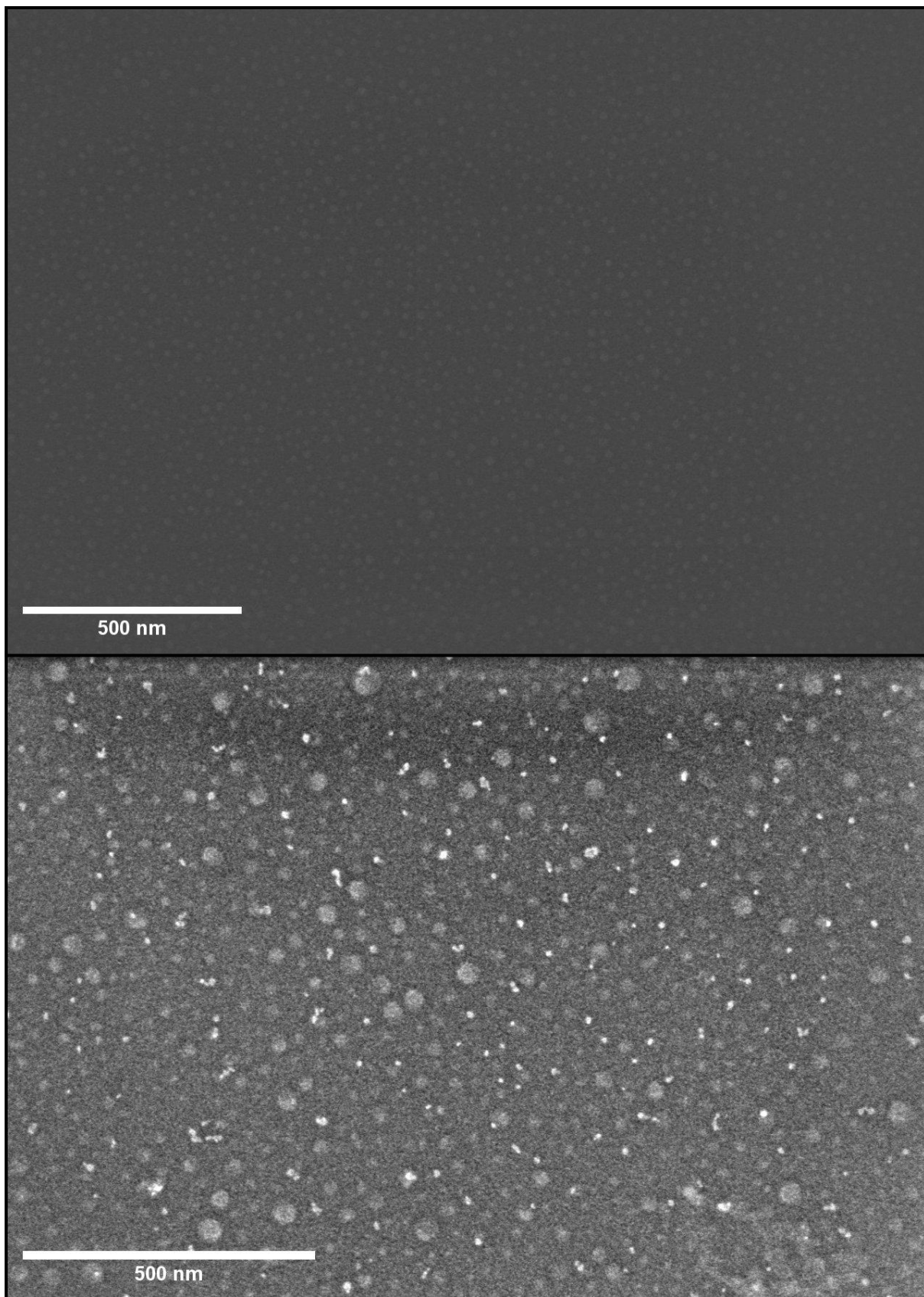


Figure 4.10: SEM images of PEG₂₀₀₀PLGA (a) and PEG₅₀₀₀PLGA (b)

The hydrodynamic diameter of PEG₂₀₀₀PLGA polymer increased by approximately 60nm, whereas the hydrodynamic radius of PEG₅₀₀₀PLGA increased by approximately 20nm when IONPs were added. Attributed to the fact that PNPs with higher molecular weight were closer to their essential nano sizes and their formation didn't incorporate most of the IONPs with the reaction speed in comparison to the smaller bare PNPs (having more capacity to form a layer around IONPs) of lower molecular weight polymer. Both polymers had uncoated IONPs, which were eliminated using centrifugal washing and magnetic separation as uncoated IONPs possess somewhat superior magnetic characteristics as described in Chapter 3. The STEM pictures revealed the presence of a layer on the IONPs when observed in SEM mode, whereas TEM mode displayed a structure consisting of a shell and core for the polymer and IONPs. Despite the lack of uniformity in the coatings or integration, we can ascertain by a comparison of SEM and TEM pictures that even individual particles exhibited some degree of polymer coating. To enhance the uniformity of this process, one can employ alternate flow rates for the FNP process, hence allowing additional time for the formation of homogenous polymer structures. The hydrophobic IONPs were rendered stable by the introduction of polymers, as confirmed by the zeta potential investigations conducted in section 4.3.1.2. Block copolymers without any surfactants were determined to be essential in the dispersibility and stability of the IONPs during FNP.

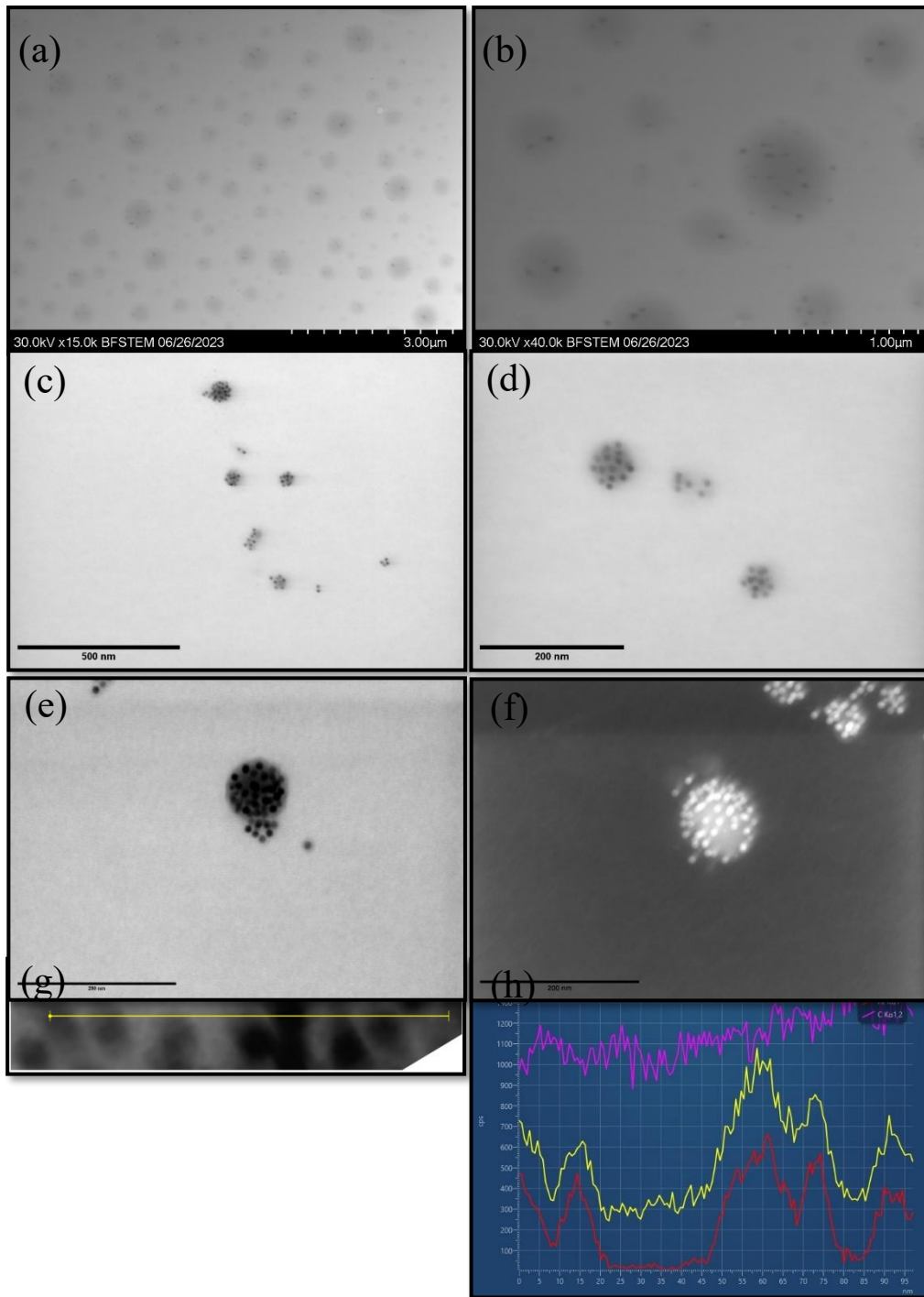


Figure 4.11: (a, b, c, d, e, f) TEM images showcasing the attachments of polymer with IONPs, and (g,h) EDX spectrum confirming iron oxide particles presence with the polymer

CHAPTER 5: CONCLUSIONS

We synthesized two PEG-PLGA polymers with distinct molecular weights to ensure a balanced ratio of PLA to PGA. The degradation potential of these polymers is maximized when the proportions of lactide and glycolide are equal, rather than having an imbalance favoring one over the other. The utilization of Sn(Oct)₂ was expanded as employed in conjunction with two distinct molecular weights of mPEG as macroinitiators for the ROP processes. This resulted in a consolidated approach to producing mPEG-PLGA with varying molecular weights. The method gave reproducible outcomes, using a standardized temperature, and reaction time with minimal formation of byproducts.

To develop an ideal carrier for drug delivery purposes, iron oxide nanoparticles were produced using iron oleate as a precursor. These nanoparticles possess magnetic properties that can be effectively utilized in combination with polymer features, resulting in the creation of an optimal carrier. First, the synthesized polymers PEG₂₀₀₀PLGA and PEG₅₀₀₀PLGA were utilized in the fabrication of bare polymeric NPs through the FNP process. The sizes of the nanoparticles did vary with the weight percentages of polymers and different MW polymers gave different sizes. Surface charge tests based on zeta potential values revealed that bare PEG-PLGA NPs synthesized using MIVM remained stable for more than 10 days and did not incur any aggregations or Ostwald ripening.

The IONPs were mixed with polymer solutions to investigate the potential of coating hydrophobic IONPs, leveraging their distinct features as an ideal drug carrier. For the FNP procedure to produce IONPs incorporated PNPs, the same requirements were applied as for bare PNPs. However, there was a lack of homogeneity in terms of size distribution in this scenario. We effectively accomplished the isolation of IONPs by utilizing polymer attachment. This was evident in S(T)EM imaging, where even a solitary iron nanoparticle exhibited a polymer coating. However, the resultant structures exhibited a lack of homogeneity in terms of the number of iron oxide particles present within each polymer structure. The observed outcomes might be ascribed to the fast mixing employed and the IONPs concentration used for the experiments, which impedes the even integration of IONPs inside the polymers due to the quick formation and enlargement of polymeric NPs. Furthermore, the attachment of IONPs to

the inner part of the polymeric NPs had a positive impact on their durability, making them highly promising for usage in drug delivery applications.

5.1 Future Recommendations:

- The findings of this study demonstrate that PEGPLGA of varying molecular weights can be synthesized using a standardized procedure, resulting in a nearly equal ratio of PLA to PGA. However, achieving an exact 50:50 ratio requires more precise control over the amounts of precursors and the percentage of catalyst, which is difficult to achieve as the quantities in question are on a micro-scale, ensuring a consistent process.
- Here a constant is applied to multiple variables, such as solvent type and flow rates, in various FNP processes. These processes range from creating bare PNPs to inserting IONPS in polymeric particles. This has led to a certain level of unpredictability in the results. Further optimization, especially with the flow rates and iron oxide concentrations is required, with a primary emphasis on attaining uniformity in combining IONPs into PNPs.
- The subsequent stages in the drug delivery applications would involve incorporating additional pharmaceuticals such as Paclitaxel into the polymer-coated IONPs, hence facilitating the creation of multifunctional NPs. By comprehending the drug loading of the block-copolymer incorporating IONPs in the flash nanoprecipitation FNP process, the particle can be readily modified to accommodate specific applications that should be examined for in vitro and in vivo studies. The application of theranostic nanoparticles can encompass the release through heat treatment, targeting capabilities, contrast imaging, and enhanced circulation times.

REFERENCES

1. Zhao, Y.-Z., et al., *Potential and problems in ultrasound-responsive drug delivery systems*. 2013: p. 1621-1633.
2. Jain, K.K.J.D.d.s., *Drug delivery systems-an overview*. 2008: p. 1-50.
3. Hall, M. and P. McCarron, *Pharmaceutical nanotechnology*, in *Encyclopedia of Nanoscience and Nanotechnology*. 2004, American Scientific Publishers. p. 469-487.
4. Sharma, S., et al., *PLGA-based nanoparticles: A new paradigm in biomedical applications*. *TrAC Trends in Analytical Chemistry*, 2016. **80**: p. 30-40.
5. Duncan, R., H. Ringsdorf, and R.J.P.T.I. Satchi-Fainaro, *Polymer therapeutics: Polymers as drugs, drug and protein conjugates and gene delivery systems: Past, present and future opportunities*. 2006: p. 1-8.
6. Xi, X., *Ligand-Installed Polymeric Nanocarriers for Combination Chemotherapy*. 2020.
7. Owens III, D.E. and N.A.J.I.j.o.p. Peppas, *Opsonization, biodistribution, and pharmacokinetics of polymeric nanoparticles*. 2006. **307**(1): p. 93-102.
8. Locatelli, E. and M.J.J.o.N.R. Comes Franchini, *Biodegradable PLGA-b-PEG polymeric nanoparticles: synthesis, properties, and nanomedical applications as drug delivery system*. 2012. **14**: p. 1-17.
9. Cleveland, M.v., et al., *New polyethylene glycol laxative for treatment of constipation in adults: a randomized, double-blind, placebo-controlled study*. 2001. **94**(5): p. 478-481.
10. Greenwald, R.B., et al., *Effective drug delivery by PEGylated drug conjugates*. 2003. **55**(2): p. 217-250.
11. Gref, R., et al., *Biodegradable long-circulating polymeric nanospheres*. 1994. **263**(5153): p. 1600-1603.
12. Bazile, D., et al., *Stealth Me. PEG-PLA nanoparticles avoid uptake by the mononuclear phagocytes system*. 1995. **84**(4): p. 493-498.
13. Huh, K.M., Y.W. Cho, and K.J.D.D.T. Park, *PLGA-PEG block copolymers for drug formulations*. 2003. **3**(5): p. 42-44.
14. Fessi, H., et al., *Nanocapsule formation by interfacial polymer deposition following solvent displacement*. 1989. **55**(1): p. R1-R4.

15. Liu, Y., et al., *Formulation of nanoparticles using mixing-induced nanoprecipitation for drug delivery*. 2019. **59**(9): p. 4134-4149.
16. Rivas, C.J.M., et al., *Nanoprecipitation process: From encapsulation to drug delivery*. 2017. **532**(1): p. 66-81.
17. Beck-Broichsitter, M., et al., *Preparation of nanoparticles by solvent displacement for drug delivery: a shift in the “ouzo region” upon drug loading*. 2010. **41**(2): p. 244-253.
18. Tao, J., S.F. Chow, and Y.J.A.p.s.B. Zheng, *Application of flash nanoprecipitation to fabricate poorly water-soluble drug nanoparticles*. 2019. **9**(1): p. 4-18.
19. Zeng, Z., et al., *Scalable production of therapeutic protein nanoparticles using flash nanoprecipitation*. 2019. **8**(6): p. 1801010.
20. Saad, W.S. and R.K.J.N.T. Prud'homme, *Principles of nanoparticle formation by flash nanoprecipitation*. 2016. **11**(2): p. 212-227.
21. Sharma, A., et al., *Magnetic Nanoparticles to Unique DNA Tracers: Effect of Functionalization on Physico-chemical Properties*. *Nanoscale Res Lett*, 2021. **16**(1): p. 24.
22. Momtazi, L., et al., *Synthesis, characterization, and cellular uptake of magnetic nanocarriers for cancer drug delivery*. 2014. **433**: p. 76-85.
23. Berzelius, J.J.J.J.ü.d.F.d.p.d.W., *Isomerie, Unterscheidung von damit analogen Verhältnissen*. 1833. **12**: p. 63-67.
24. *Introduction*, in *Principles of Polymerization*. 2004. p. 1-38.
25. Hamid Akash, M.S., K. Rehman, and S.J.P.R. Chen, *Natural and synthetic polymers as drug carriers for delivery of therapeutic proteins*. 2015. **55**(3): p. 371-406.
26. Kricheldorf, H.R., *Handbook of polymer synthesis*. Vol. 24. 1991: CRC press.
27. Obi, B.E., *Polymeric Foams Structure-Property-Performance*. 2018, Elsevier.
28. Cowie, J.M.G. and V. Arrighi, *Polymers: chemistry and physics of modern materials*. 2007: CRC press.
29. McKeen, L.W., *The Effect of Creep and Other Time Related Factors on Plastics and Elastomers* Elsevier, 2009: p. 1-41.
30. Coleman, M.M., *Fundamentals of polymer science: An introductory text*. . Routledge., 2019.

31. Yokoyama, M.J.C.r.i.t.d.c.s., *Block copolymers as drug carriers*. 1992. **9**(3-4): p. 213-248.
32. Letchford, K., H.J.E.j.o.p. Burt, and biopharmaceutics, *A review of the formation and classification of amphiphilic block copolymer nanoparticulate structures: micelles, nanospheres, nanocapsules and polymersomes*. 2007. **65**(3): p. 259-269.
33. Agrahari, V. and V.J.D.D.T. Agrahari, *Advances and applications of block-copolymer-based nanoformulations*. 2018. **23**(5): p. 1139-1151.
34. Danafar, H.J.D.r., *Applications of copolymeric nanoparticles in drug delivery systems*. 2016. **66**(10): p. 506-519.
35. Jhaveri, A.M. and V.P.J.F.i.p. Torchilin, *Multifunctional polymeric micelles for delivery of drugs and siRNA*. 2014. **5**: p. 77.
36. Matsuo, Y., et al., *Precise synthesis of block polymers composed of three or more blocks by specially designed linking methodologies in conjunction with living anionic polymerization system*. 2013. **5**(3): p. 1012-1040.
37. Aoshima, S. and S.J.C.R. Kanaoka, *A renaissance in living cationic polymerization*. 2009. **109**(11): p. 5245-5287.
38. Feng, H., et al., *Block copolymers: Synthesis, self-assembly, and applications*. 2017. **9**(10): p. 494.
39. Webster, O.W.J.N.S.M., *Group transfer polymerization: a critical review of its mechanism and comparison with other methods for controlled polymerization of acrylic monomers*. 2004: p. 1-34.
40. Hadjichristidis, N., et al., *Block copolymers by ring opening metathesis polymerization*. 2003: p. 80-90.
41. Doppalapudi, S., et al., *Biodegradable polymers for targeted delivery of anti-cancer drugs*. 2016. **13**(6): p. 891-909.
42. Lipinski, C.J.A.P.R., *Poor aqueous solubility—an industry wide problem in drug discovery*. 2002. **5**(3): p. 82-85.
43. Goldberg, M., R. Langer, and X.J.J.o.B.S. Jia, Polymer Edition, *Nanostructured materials for applications in drug delivery and tissue engineering*. 2007. **18**(3): p. 241-268.
44. Bobbala, S., S.D. Allen, and E.A.J.N. Scott, *Flash nanoprecipitation permits versatile assembly and loading of polymeric bicontinuous cubic nanospheres*. 2018. **10**(11): p. 5078-5088.
45. Johnson, B.K. and R.K.J.A.J. Prud'homme, *Chemical processing and micromixing in confined impinging jets*. 2003. **49**(9): p. 2264-2282.

46. Pinkerton, N.M., et al., *Formation of stable nanocarriers by in situ ion pairing during block-copolymer-directed rapid precipitation*. 2013. **10**(1): p. 319-328.
47. D'Addio, S.M., et al., *Effects of block copolymer properties on nanocarrier protection from in vivo clearance*. 2012. **162**(1): p. 208-217.
48. Pucci, A., et al., *Click chemistry on the surface of PLGA-b-PEG polymeric nanoparticles: a novel targetable fluorescent imaging nanocarrier*. 2013. **15**: p. 1-6.
49. Pustulka, K.M., et al., *Flash nanoprecipitation: particle structure and stability*. 2013. **10**(11): p. 4367-4377.
50. Bhatt, P., et al., *Polymers in drug delivery: an update*, in *Applications of polymers in drug delivery*. 2021, Elsevier. p. 1-42.
51. Li, S. and S.J.M. McCarthy, *Influence of crystallinity and stereochemistry on the enzymatic degradation of poly (lactide) s*. 1999. **32**: p. 4454-4456.
52. Jeong, J.H., et al., *Synthesis, characterization and protein adsorption behaviors of PLGA/PEG di-block co-polymer blend films*. 2000. **18**(3-4): p. 371-379.
53. Xue, Y.-N., et al., *Synthesis and self-assembly of amphiphilic poly (acrylic acid-b-DL-lactide) to form micelles for pH-responsive drug delivery*. 2009. **50**(15): p. 3706-3713.
54. Little, A., et al., *Synthesis of poly (Lactic acid-co-glycolic acid) copolymers with high glycolide ratio by ring-opening polymerisation*. 2021. **13**(15): p. 2458.
55. Pulingam, T., et al., *Exploring various techniques for the chemical and biological synthesis of polymeric nanoparticles*. 2022. **12**(3): p. 576.
56. Mitchell, M.J., et al., *Engineering precision nanoparticles for drug delivery*. 2021. **20**(2): p. 101-124.
57. Lee, V.E., et al., *Flash nano-precipitation and-complexation to produce polymer colloids*. 2019. **9**: p. 61.
58. LaMer, V.K. and R.H.J.J.o.t.a.c.s. Dinegar, *Theory, production and mechanism of formation of monodispersed hydrosols*. 1950. **72**(11): p. 4847-4854.
59. Valente, I., et al., *Nanoprecipitation in confined impinging jets mixers: Production, characterization and scale-up of pegylated nanospheres and nanocapsules for pharmaceutical use*. 2012. **77**: p. 217-227.
60. Sharratt, W.N., et al., *Precision polymer particles by flash nanoprecipitation and microfluidic droplet extraction*. 2021. **3**(10): p. 4746-4768.

61. D'Addio, S.M. and R.K.J.A.d.d.r. Prud'homme, *Controlling drug nanoparticle formation by rapid precipitation*. 2011. **63**(6): p. 417-426.
62. Liu, Y., et al., *Mixing in a multi-inlet vortex mixer (MIVM) for flash nano-precipitation*. 2008. **63**(11): p. 2829-2842.
63. Agrahari, V., V. Agrahari, and A.K.J.T.d. Mitra, *Nanocarrier fabrication and macromolecule drug delivery: challenges and opportunities*. 2016. **7**(4): p. 257-278.
64. Agrahari, V., et al., *Composite nanoformulation therapeutics for long-term ocular delivery of macromolecules*. 2016. **13**(9): p. 2912-2922.
65. Zhu, Z.J.B., *Effects of amphiphilic diblock copolymer on drug nanoparticle formation and stability*. 2013. **34**(38): p. 10238-10248.
66. Zhang, D., et al., *Drug-loaded PEG-PLGA nanoparticles for cancer treatment*. 2022. **13**: p. 990505.
67. Marcu, A., et al., *Magnetic iron oxide nanoparticles as drug delivery system in breast cancer*. 2013. **281**: p. 60-65.
68. Maharramov, A.M., et al., *IRON OXIDE NANOPARTICLES IN DRUG DELIVERY SYSTEMS*. 2011. **6**(2).
69. Modak, M., et al., *Magnetic nanostructure-loaded bicontinuous nanospheres support multicargo intracellular delivery and oxidation-responsive morphological transitions*. 2020. **12**(50): p. 55584-55595.
70. Fuller, E.G., et al., *Externally triggered heat and drug release from magnetically controlled nanocarriers*. 2019. **1**(2): p. 211-220.
71. Panda, J., et al., *Engineered polymeric iron oxide nanoparticles as potential drug carrier for targeted delivery of docetaxel to breast cancer cells*. 2019. **485**: p. 165-173.
72. Kato, N., et al., *Enzyme reaction controlled by magnetic heating due to the hysteresis loss of γ -Fe₂O₃ in thermosensitive polymer gels immobilized β -galactosidase*. 1998. **6**(4): p. 291-296.
73. Simpson, C.R., et al., *Near-infrared optical properties of ex vivo human skin and subcutaneous tissues measured using the Monte Carlo inversion technique*. 1998. **43**(9): p. 2465.
74. Marinelli, L., et al., *Preparation, characterization, and biological evaluation of a hydrophilic peptide loaded on PEG-PLGA nanoparticles*. 2022. **14**(9): p. 1821.
75. Park, J., et al., *Ultra-large-scale syntheses of monodisperse nanocrystals*. 2004. **3**(12): p. 891-895.

76. Bandyopadhyay, S., et al., *Hydrophobic Iron Oxide Nanoparticles: Controlled Synthesis and Phase Transfer via Flash Nanoprecipitation*. 2024.
77. Ježková, M., et al., *The preparation of mono-and multicomponent nanoparticle aggregates with layer-by-layer structure using emulsion templating method in microfluidics*. 2022. **247**: p. 117084.
78. Singh, M., et al., *Chapter 14—Nuclear magnetic resonance spectroscopy*. 2022: p. 321-339.
79. Jörger, M. and G. Zachmann, *The New Vacuum Ft-Ir Spectrometer: Design Advances and Research Application*. 2007.
80. Petit, S. and J. Madejova, *Fourier transform infrared spectroscopy*, in *Developments in clay science*. 2013, Elsevier. p. 213-231.
81. Holmes, J., et al., *Surface functionalization strategies for monolayer doping*. 2018.
82. Ramachandran, V.S. and J.J. Beaudoin, *Handbook of analytical techniques in concrete science and technology: principles, techniques and applications*. 2000: Elsevier.
83. Varela, M., et al., *Materials characterization in the aberration-corrected scanning transmission electron microscope*. 2005. **35**: p. 539-569.
84. Zanetti-Ramos, B.G., et al., *Dynamic light scattering and atomic force microscopy techniques for size determination of polyurethane nanoparticles*. 2009. **29**(2): p. 638-640.
85. Ma, J., et al., *Application of gel permeation chromatography technology in asphalt materials: A review*. 2021. **278**: p. 122386.
86. Qian, H., et al., *A strategy for control of “random” copolymerization of lactide and glycolide: application to synthesis of PEG-b-PLGA block polymers having narrow dispersity*. 2011. **44**(18): p. 7132-7140.
87. Ansary, R.H., M.B. Awang, and M.M.J.T.J.o.P.R. Rahman, *Biodegradable poly (D, L-lactic-co-glycolic acid)-based micro/nanoparticles for sustained release of protein drugs-A review*. 2014. **13**(7): p. 1179-1190.
88. Makadia, H.K. and S.J.J.P. Siegel, *Poly lactic-co-glycolic acid (PLGA) as biodegradable controlled drug delivery carrier*. 2011. **3**(3): p. 1377-1397.
89. Li, Y.-P., et al., *PEGylated PLGA nanoparticles as protein carriers: synthesis, preparation and biodistribution in rats*. 2001. **71**(2): p. 203-211.
90. Zhen, G., et al., *Comparative study of the magnetic behavior of spherical and cubic superparamagnetic iron oxide nanoparticles*. 2011. **115**(2): p. 327-334.

91. Salem, N.M., et al., *New route for synthesis magnetite nanoparticles from ferrous ions and Pistachio leaf extract*. 2013. **3**(3): p. 48-51.
92. Glasgow, W., et al., *Continuous synthesis of iron oxide (Fe₃O₄) nanoparticles via thermal decomposition*. 2016. **26**: p. 47-53.
93. Zhang, J., et al., *Preparation and characterization of polymeric micelles from poly (D, L-lactide) and methoxypolyethylene glycol block copolymers as potential drug carriers*. 2007. **12**(4): p. 493-496.
94. Galindo-Rodriguez, S., et al., *Physicochemical parameters associated with nanoparticle formation in the salting-out, emulsification-diffusion, and nanoprecipitation methods*. 2004. **21**: p. 1428-1439.
95. Shen, H., et al., *Self-assembling process of flash nanoprecipitation in a multi-inlet vortex mixer to produce drug-loaded polymeric nanoparticles*. 2011. **13**: p. 4109-4120.
96. Ansell, S.M., et al., *Modulating the therapeutic activity of nanoparticle delivered paclitaxel by manipulating the hydrophobicity of prodrug conjugates*. 2008. **51**(11): p. 3288-3296.
97. Johnson, B.K. and R.K.J.P.r.l. Prud'homme, *Mechanism for rapid self-assembly of block copolymer nanoparticles*. 2003. **91**(11): p. 118302.